FACULTY OF INFORMATION TECHNOLOGY AND ELECTRICAL ENGINEERING
DEGREE PROGRAMME IN ELECTRONICS AND COMMUNICATIONS ENGINEERING

MASTER'S THESIS

FIBER OPTIC PIGTAILING AND PACKAGING OF PHOTONIC INTEGRATED CIRCUITS

Author	Markus Schröder
Supervisor	Anssi Mäkynen
Second Examiner	Ville Kaikkonen
Technical Advisor	Mikko Karppinen

May 2023

Schröder M. (2023) Fiber Optic Pigtailing and Packaging of Photonic Integrated Circuits. University of Oulu, Faculty of Information Technology and Electrical Engineering, Degree Programme in Electronics and Communications Engineering, 43 p.

ABSTRACT

This work studies a coupling method and resulting coupling losses of a photonics module composed of a silicon-on-insulator (SOI) photonic integrated circuit, a 16-channel single mode fiber array and a spot size converter chip. The converter chip is used to optimize the coupling efficiency between the fiber array and the SOI circuit by matching the mode field diameter of the fiber array to that of the SOI circuit. The SOI circuit has multiple 180° loop waveguides to facilitate active alignment by optical loss measurements through edge coupling during assembly. The SOI circuit is attached to a copper plate with a printed circuit board.

The input and output couplings of the converter chip were made up using the active alignment method, a 1536 nm super luminescent light emitting diode (SLED) as a light source, an ultraviolet light curable adhesive and a computer controlled high precision alignment and assembly station. As a result, light travels through the fiber array and the spot size converter to the 180° optical loops on the SOI circuit and after that back to the fiber array through the spot size converter. The goal of this work was coupling loss of less than 4.5 decibels measured through a loop of the finished module. The coupling losses of the best and worst loops of the module were measured to be 4.4 dB and 7.9 dB, respectively. Possible reasons for the high coupling loss difference between the loops were concluded to be the inaccuracy in the waveguide facet polishing angles on the spot size converter chip, worn-out fiber connector and misalignment caused by the shrinking of the adhesive during curing.

Key words: edge coupling, fiber array, spot size converter, waveguide, SOI.

Schröder M. (2023) Kuituhännöitys ja integroidun fotoniikan paketointi. Oulun yliopisto, tieto- ja sähkötekniikan tiedekunta, elektroniikan ja tietoliikennetekniikan tutkinto-ohjelma. Diplomityö, 43 p.

TIIVISTELMÄ

Tässä työssä tutkitaan kytkentämenetelmää ja siitä aiheutuvia kytkentähäviöitä fotoniikkamoduulissa, joka koostuu integroidusta silicon-on-insulator (SOI) piiristä, 16-kanavaisesta yksimuotokuiturivistä ja spottikoon muunninsirusta. Muunninsirua käytetään optimoimaan kuiturivin ja SOI-piirin välinen kytkentätehokkuus sovittamalla kuiturivin kuiduissa ja SOI-piirissä etenevät muotokentät toisiinsa. SOI-piirissä on useita 180 asteen silmukkavalokanavia, jotka helpottavat aktiivista kohdistusta optisen häviömittauksen avulla kokoonpanon aikana. SOI-piiri on kiinnitetty kuparilevyyn piirilevyn kanssa.

Muunninsirun tulo- ja lähtökytkennät tehtiin käyttämällä aktiivista kohdistusmenetelmää, valonlähteenä 1536 nm:n superluminesenssi lediä (SLED), ultraviolettivalolla kovettuvaa liimaa sekä tietokoneohjattua erittäin tarkkaa kohdistus- ja kokoonpanoasemaa. Tämän seurauksena valo kulkee kuiturivin ja muunninsirun läpi SOI-piirin 180° optisiin silmukoihin ja sen jälkeen takaisin kuituriviin muunninsirun kautta. Tämän työn tavoitteena oli alle 4,5 desibelin kytkentähäviö mitattuna valmiin moduulin silmukasta. Moduulin parhaan ja huonoimman silmukan kytkentähäviöiksi mitattiin 4,4 dB ja 7,9 dB. Mahdollisia syitä silmukoiden väliseen suureen kytkentähäviöeroon pääteltiin olevan epätarkkuudet muunninsirun valokanavien päiden kiillotuskulmissa, kulunut kuituliitin ja liiman kutistumisesta kovettumisen aikana aiheutunut kohdistusvirhe.

Avainsanat: reunakytkentä, kuiturivi, spottikoon muunninsiru, valokanava, silicon-on insulator.

TABLE OF CONTENTS

ABSTRACT
TIIVISTELMÄ
TABLE OF CONTENTS
FOREWORD
LIST OF ABBREVIATIONS AND SYMBOLS
1 INTRODUCTION 8
2 SINGLE MODE FIBER TO SINGLE MODE WAVEGUIDE COUPLING 10
2.1 Single mode fiber array 12
2.2 Coupling the spot size converter chip 13
3 COUPLING PROCESS 18
3.1 Tools 18
3.2 Alignment process 20
3.2.1 Aligning fiber array to spot size converter 21
3.2.2 Aligning spot size converter to photonic integrated circuit 29
3.3 Final assembly and measurements 31
4 DISCUSSION 33
5 SUMMARY 38
6 REFERENCES 39
7 APPENDICES 40

FOREWORD

This work was made for VTT Oulu Photonics and RF Integration team. The purpose of this work was to improve the development process of packaging fiber optic modules. Packaging is made by pigtailing to photonic integrated circuits manufactured in VTT. Fabrication of photonic integrated circuits is made in VTT Espoo, and the photonic assembly is made in VTT Oulu.

I would like to thank my thesis supervisors and technical advisors Anssi Mäkynen, Ville Kaikkonen, Mikko Karppinen, Aila Sitomaniemi, and many other researchers who have helped me in this work at VTT.

Oulu, May 3, 2023

Markus Schröder

LIST OF ABBREVIATIONS AND SYMBOLS

CMOS	complementary metal-oxide semiconductor
DI	deionized
FA	fiber array
InGaAs	indium gallium arsenide
IPA	isopropanol alcohol
IR	infrared
MPW	multi-project wafer
OSA	optical spectrum analyser
PCB	printed circuit board
PIC	photonic integrated circuit
PM	polarization maintaining
SLED	super luminescent light emitting diode
SM	single mode
SMF	single mode fiber
SSC	spot size converter
SOI	silicon-on-insulator
TIA	transimpedance amplifier
Thin-film SOI	silicon on insulator technology with < 1 µm waveguide thickness
Thick-film SOI	silicon on insulator technology with > 1 µm waveguide thickness
TM	transverse magnetic
TE	transverse electric
UV	ultraviolet
WG	waveguide
a	air gap distance on some x-coordinate
b	air gap distance on x coordinate different than a
c	difference between a and b x-coordinates
d	diameter
M	maximum number of core guided modes
n	refractive Index
P_m	measured optical power from the device
P_{ref}	measured optical power from the reference
dB	decibel
mW	milliwatt
m°	millidegree
nm	nanometer
nW	nanowatt
W	watt
µm	micrometer
µW	microwatt
°	degree
°C	Celsius degree
α_{Air}	angle in pitch without adhesive
α_{Glue}	angle in pitch with adhesive

α_{Roll}	rotation in roll
α_{Yaw}	rotation in yaw
α_{Error}	amount of error from 90-degree angle in degrees
θ	bounce angle
λ	wavelength

1 INTRODUCTION

Photonic integrated circuits (PICs) are like electrical integrated circuits but instead of electrical current paths chips have waveguides (WGs) which make paths for light. Different optical devices and components can be implemented on a single chip that can generate, focus, split, combine, isolate, polarize, couple, switch, modulate and detect light [1].

For light to propagate confined inside a medium, the medium must have higher refractive index than the medium surrounding it. The medium where the light is supposed to travel is called the core, and the medium surrounding the core is called the cladding [2]. This is the structure of a fiber optic cable. The light stays confined inside the cable because of total internal reflection. Because fiber optic cables have low optical losses, they can carry light signals across oceans. In PICs it is desirable to have a larger refractive index contrast between the core and cladding than fiber optic cables have. This enables the waveguides to have smaller bending radii and smaller core dimensions compared with an optical fiber. The downside of large refractive index contrast is that it makes the waveguides more wavelength dependent and more sensitive to geometric variations [3, 4].

Silicon-on-insulator (SOI) is a common wafer material platform in integrated photonics because of its low absorption in wavelengths commonly used in telecommunications (1310 nanometer (nm) to 1550 nm) [5]. SOI also has higher refractive index contrast than other material systems commonly used in integrated photonics, and it is compatible with complementary metal-oxide semiconductor (CMOS) manufacturing processes [6]. PICs are often fabricated in multi project wafer runs (MPWs), which means that there can be different chips with different chip designs on the same silicon wafer. This allows companies buy only a fraction of the wafer area and no need for committing to a full wafer run [7].

SOI PICs are commonly used in tele- and data communications. Integration of photonic and electronic circuits allows more complex communication networks with unique functionality [3]. Compared with discrete components, the integration of photonic circuits has the same benefits as with the integration of electronic circuits, which are improvements in reliability and functionality and lower costs [3]. Modules that have integrated photonics and fiber optic cables also tend to be lighter than modules that have electronic integrated circuits and copper cables. This is an advantage for example in space and aviation applications.

This work is focused on thick-film SOI PICs, which refers to 1 micrometer (μm) and above thick SOI waveguides. These PICs are manufactured at VTT. The PICs have a SOI thickness of ~3 μm and ~11 μm. Spot size converter chips have larger SOI thickness because they are used to match the modes of a single mode (SM) fiber array (FA) to the ~3 μm SOI PIC waveguide mode. Thin-film SOI (1 μm and thinner) would have smaller PIC footprint and smaller bending radii, but it is more sensitive to high powers and polarization. The fabrication of thin-film SOI is also more expensive and the tolerances are tighter. Also, the coupling to SM fibers is more difficult due to the larger difference in modes compared with thick-film SOI coupling to SM fibers.

The scope of this thesis was improving the process of packaging a module with low loss coupling from a fiber array to a SOI PIC. Coupling loss of less than 4.5 decibels measured through a loop is desired and it should also stay stable when the module is used. A demonstration was made through a prototype assembly with PIC-based test chip. The task was challenging because of the requirement of robust alignment of FA with multiple channels to the SOI PIC with submicron accuracy including the SSC in between (Figure 1).

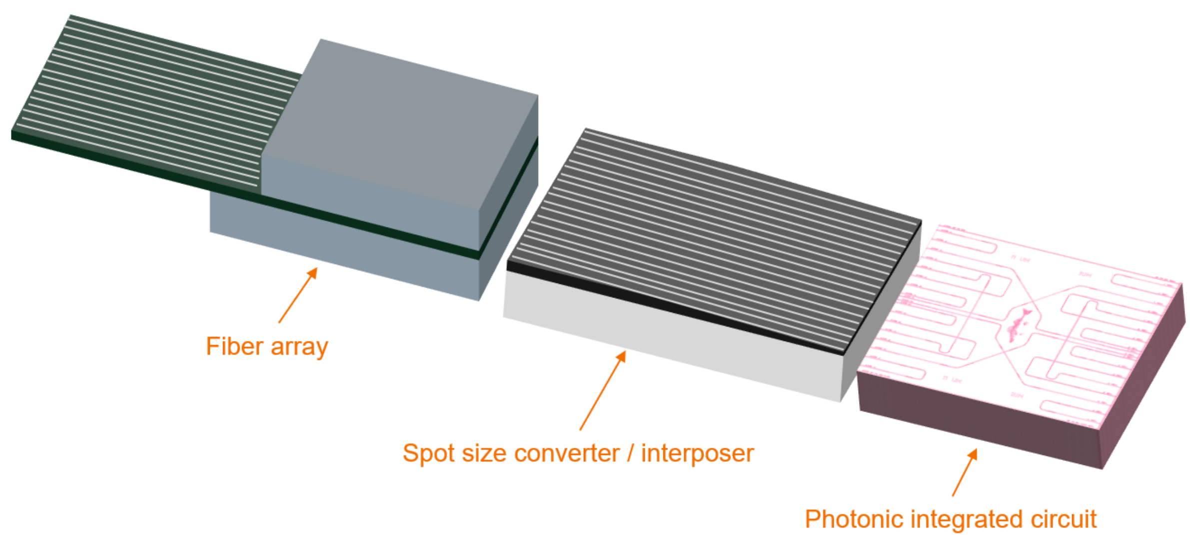

Figure 1. Coupling from fiber array through spot size converter to photonic integrated circuit. (Not in scale.)

The status of this development process at the beginning of this work was that coupling a fiber array to PIC directly without the spot size converter was successful. Only the stability of assemblies including also electrical contacts was not found to be sufficient. Coupling losses of the spot size converters had been measured with different measurement setups and spectrum analysers were not used then. Also, some assemblies had been made with the spot size converters, but the stability in modules enabling also electrical contacts was not good enough. The difficulties in photonic packaging cause a bottleneck in the development of commercially relevant integrated photonic devices [8].

The development of this pigtailing process has been going on for a few years at VTT before this work started and multiple ways of doing the process has been developed by several individual researchers. Some of the earlier developed methods are used as such in this work. The less accurate but fast methods, for example, were used for initial alignment. Most of the fine alignment methods, however, were developed by the author to achieve better alignment accuracy than what would have been possible with the earlier methods. Though author has had the major role in developing the pigtailing process supervisor, fellow researchers, and technicians have given indispensable help with their implementation. Also, most of the preparations needed for the assembly to the point that it could be pigtailed has been done by other people.

This work consists of a brief introduction to fiber optics, some examples of pigtailing technologies, introduction to the used equipment and an overview of the process steps, and finally, results, discussion, and a summary.

2 SINGLE MODE FIBER TO SINGLE MODE WAVEGUIDE COUPLING

Light propagates inside fibers and waveguides by total internal reflection. The propagation of the light can be approximated by a line bouncing in a waveguide or a fiber. This is called the ray optics model. However, this is an approximation, and for analyzing the propagation more precisely, wave optics model must be considered. Wave optics model is based on Maxwell's equations.

Patterns of transverse magnetic (TM) and transverse electric (TE) fields in waveguides are called modes. An optical fiber or a waveguide, which can carry many modes in certain wavelength range, is called as a multimode fiber or a multimode waveguide. If a fiber or a waveguide supports only one propagating confined mode in its specific wavelength range, it is called single mode fiber (SMF) or single mode (SM) waveguide (WG). All SM fibers will also start to support other modes after the wavelength of the light goes below a certain point. This point is called as the cut-off wavelength. Fibers are single mode only for core guided modes. There can be other modes called cladding modes and radiative modes. The number of core guided TE modes a fiber / waveguide can carry depend on the wavelength of the light, diameter of the core and refractive indices of the core and cladding. The maximum number of modes is

$$M = 2\frac{d}{\lambda}(n_1^2 - n_2^2)^{1/2}, \tag{1}$$

where M is the number of modes (rounded to the nearest integer), d is the diameter of the core, and λ is the wavelength, n_1 is the refractive index of the core and n_2 is the refractive index of the cladding. The coupling angle influences the number of modes, but M determines the maximum [1]. When modes are thought with ray optics model, every mode corresponds to a bounce angle θ_m

$$sin\,\theta_m = m\frac{\lambda}{2d},\ m = 1, 2,\ldots \tag{2}$$

where the corresponding field is called the mth mode [1]. Bounce angle is also illustrated in Figure 2. The first mode $m = 1$ has the smallest bounce angle θ_1 and therefore it has the highest group velocity of the modes. First order mode has its peak intensity in the center of the core. Critical angle, which is the largest angle that the waveguide can guide is

$$\theta_c = cos^{-1}\left(\frac{n_2}{n_1}\right), \tag{3}$$

where θ_c is the critical angle [1].

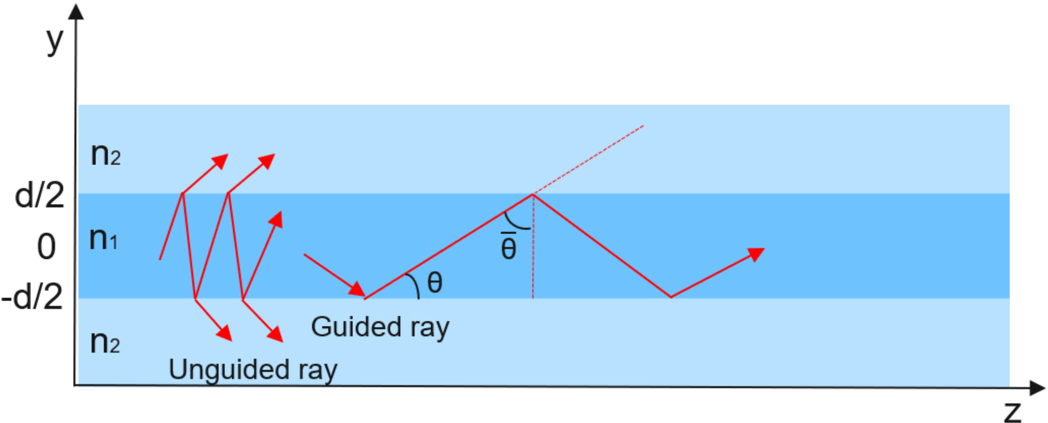

Figure 2. 2D illustration of a planar (slab) waveguide. Rays making an angle $\theta < \theta_c$ are guided by total internal reflection.

Single mode operation is desirable in telecommunications related applications. The optical power coupled into higher order modes should be minimized. Single mode fibers and waveguides have a smaller core, and therefore the mode field diameter is smaller than in multimode fibers / waveguides. To achieve good coupling between SM waveguides, both waveguides should have the same mode field diameter and they should be aligned with submicron accuracy. This makes coupling single mode fibers / waveguides more difficult than coupling multimode fibers.

Different coupling methods for fiber to PIC can be categorized in two main groups: grating coupling and edge coupling. The difference between these two methods is that in grating coupling the fiber is aligned vertically towards the chips top or bottom surface (perpendicularly to the waveguides), and in edge coupling the fiber is aligned horizontally (parallel to the waveguides). The difference is illustrated in Figure 3.

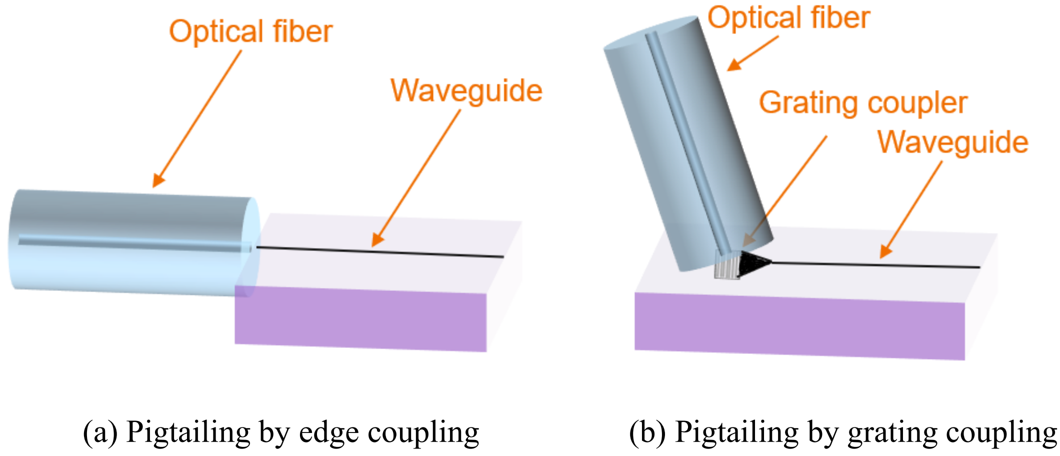

(a) Pigtailing by edge coupling (b) Pigtailing by grating coupling

Figure 3. Two different fiber optic pigtailing methods to photonic integrated circuits.

Grating coupling is based on specific pitched grating on top or bottom of the waveguide. The grating couples the light into the waveguide by diffraction. In edge coupling the PIC has a waveguide facet on the side of the PIC where a fiber is aligned to the waveguide. Grating

coupling has relatively wide alignment tolerances and the fabrication of the grating is relatively easy with lithographic methods. Edge coupling on the other hand has tighter tolerances for alignment, and it requires optical quality facets which are more difficult to fabricate. Coupling by edge coupling results in higher coupling efficiency and wider bandwidth compared with grating coupling [9]. Edge coupling can also be polarization independent and grating coupling is always polarization dependent. Only edge coupling is used in this work.

2.1 Single mode fiber array

Fiber array provides connectors where the light is coupled to the module. Fiber arrays used in this work mainly use FC/APC connectors, where the fiber end and the surrounding ferrule is polished at an angle of 8°. This minimizes back reflections from the fiber end because the back reflected light is absorbed due to the increased angle in the fiber core as can be seen in Figure 4.

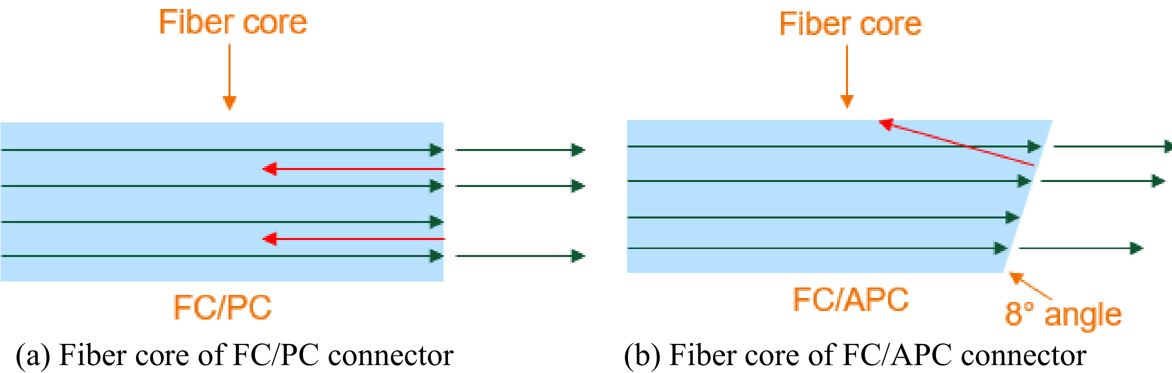

(a) Fiber core of FC/PC connector (b) Fiber core of FC/APC connector

Figure 4. Difference between FC/PC and FC/APC connectors. Reflected light is illustrated with red arrows.

FA consist of 16 connectors and optical fibers which each are one meter long. The fibers are surrounded by a protective layer of plastic called the loose tube. The purpose of the loose tube is to provide protection for the fiber inside. At the end of the fibers there is a glass part where all the fibers are glued inside in a row. The glass part is constructed from two glass pieces and the fibers are between the pieces. The bottom piece has 16 v-grooves with 250 µm pitch (distance between fiber cores) where the bare fibers are glued in place as the top part is placed on top. Figure 5 shows an illustration of a v-groove glass for 8-channel fiber arrays.

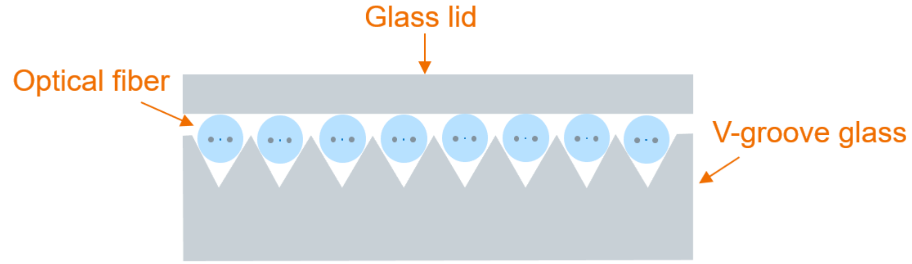

Figure 5. Illustration of the end part of a fiber array with eight fibers.

Between the loose tubes and the v-groove glass there is a 40 millimeter (mm) long section of bare fibers. From the bare fibers, strain relief can be glued to provide protection from the movements of the fibers and connectors when the module is in use.

The fibers in the fiber array are polarization maintaining (PM), which means that the polarization does not change at the output even if the fibers are bent. This is done by breaking the symmetry of the fiber by adding higher refractive index stress rods on the opposite sides of the core. That way different polarizations cannot exchange power because they have different propagation constants. Breaking the symmetry can be done in other ways too, as can be seen from Figure 6. In this work, PM fibers use Panda style PM fibers.

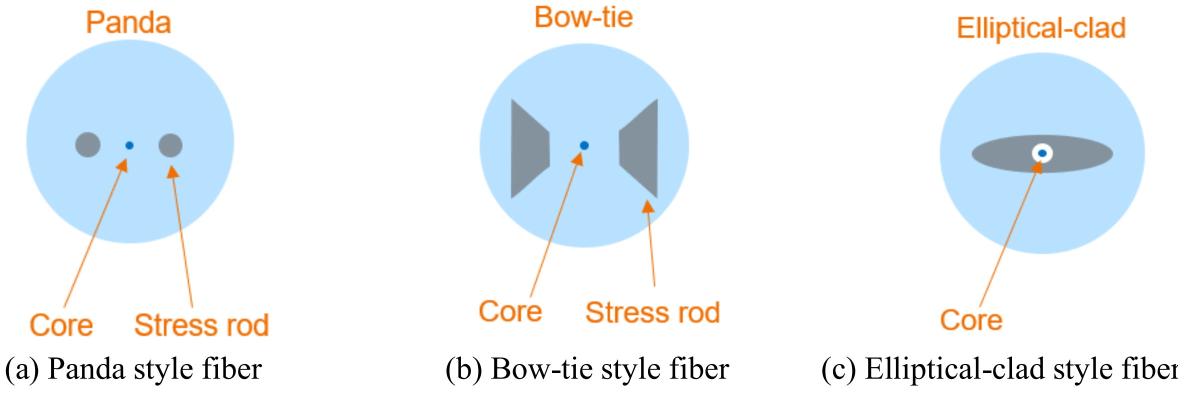

(a) Panda style fiber (b) Bow-tie style fiber (c) Elliptical-clad style fiber

Figure 6. Cross cuts of different style PM fibers.

2.2 Coupling the spot size converter chip

In this work, the module assembly includes two edge couplings. First coupling is done between a 16-channel polarization maintaining single mode fiber array and a spot size converter. The second coupling is done when already combined PM SM FA and SSC is attached to a 16-channel photonic integrated circuit. Both couplings effect on the overall optical losses of the module. Coupling multiple channel fiber arrays is more challenging than coupling of single fibers.

The spot size converter is a 11 µm SOI chip that has 20 straight channels with 250 µm pitch. Converting the spot size vertical dimension to 3 µm is done by tapering the waveguides vertically. This leads to a waveguide that is 11 µm × 11 µm on the input side, and 11 µm × 3

μm on the output side. The tapering also removes the silicon oxide cladding that is on top of the waveguides near the 3 μm end. After the chip is tapered it is coated with a thin layer of anti-reflective coating. Figure 7 is a microscope image of one of the facets in the tapered end. Figure 8 shows the other end that is 11 μm in height and has the oxide cladding still on top. Both ends are hand polished, and imperfections are usual that can be seen from Figure 8, where a corner of the waveguide has chipped. This imperfection seen in the image should not have significant effect on coupling losses though.

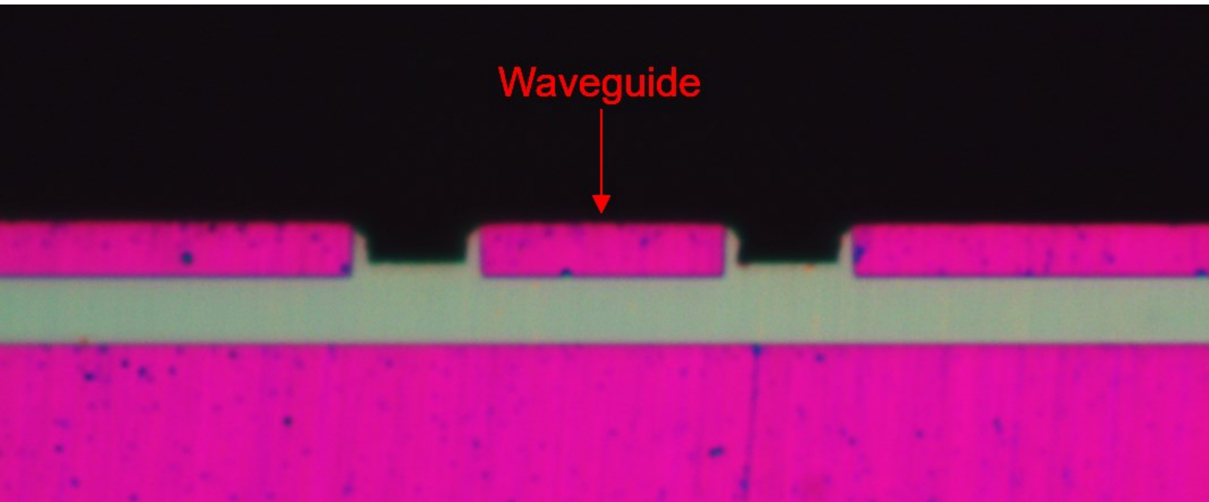

Figure 7. Microscope image of a waveguide facet of the spot size converter with 11 μm × 3 μm dimensions. This end is coupled to the SOI PIC.

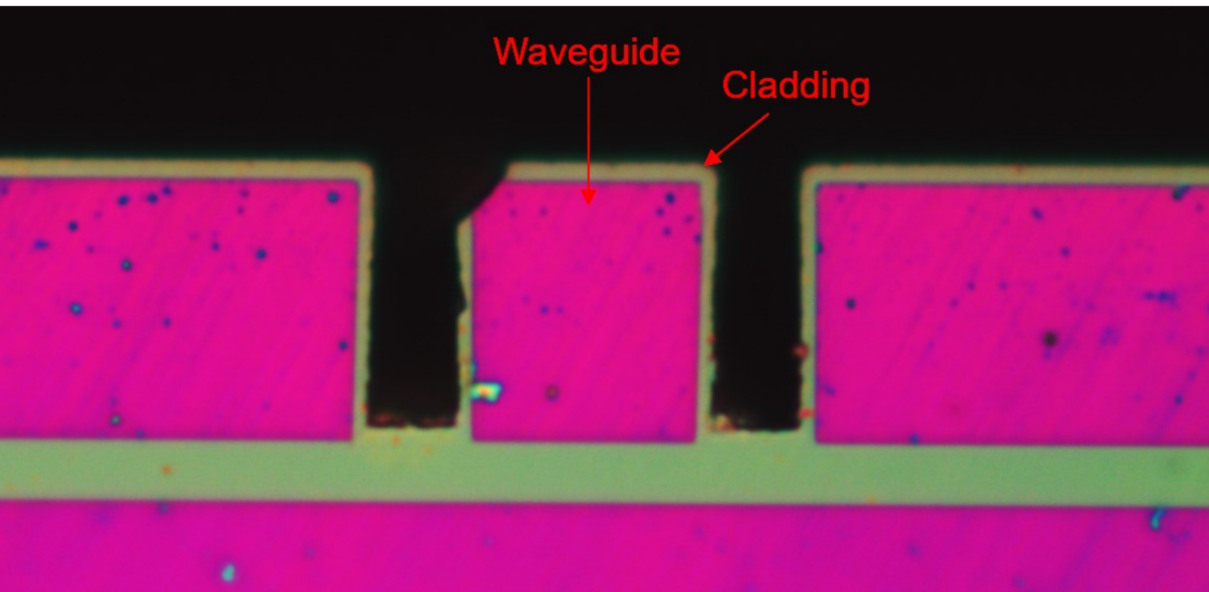

Figure 8. Microscope image of a waveguide facet of the spot size converter with 11 μm × 11 μm dimensions. This end is coupled to the fiber array.

In this work, a test SOI PIC for fiber optic pigtailing is used. The chip has been made for testing and developing the process of fiber optic pigtailing. The chip has loops of a different kind and feedthroughs on all its channels for active alignment and measurements. With this SOI

PIC active alignment is made by coupling light to a channel of the PIC and the light is detected on the output of that channel. The alignment is made then by moving the input fiber to position where the optical power detected is the highest [10]. This is illustrated with an example in Figure 9. Three different rotations of the fiber array effect on the optical power detected from the output channels, but not as much as x, y, and z directions. Two rotations (yaw and pitch) can usually be set by passive alignment with no light source. Roll rotation determines the difference between y-coordinates of channel 1 and 16 on the fiber array facets (Figure 9) and has to be set with active alignment.

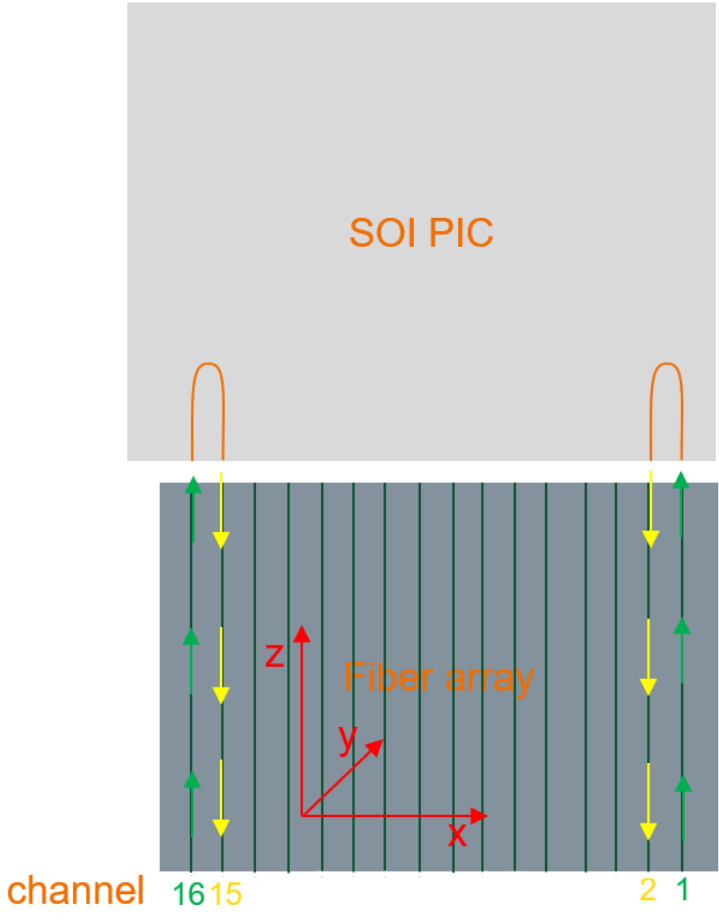

Figure 9. Active alignment is made by moving the fiber array in x, y, and z directions when the light source is connected with channel numbers 1 and 16 on the fiber array. Movements are made so that the light detected from channel numbers 2 and 15 on the fiber array achieve the maximum optical power.

Having multiple loops on a chip is useful in coupling tests because measurements can be made across the joint in comparison to functional chip, which usually have only one loop per edge of the chip. The test chip has been finished like the SSC chip by polishing the facets by hand. After polishing, the chip is coated with the same anti-reflective coating that is used with the SSC chip. The test PIC has facets with dimensions 11 µm × 3 µm that match with the other end of the SSC chip. The sides of this test PIC are identical except the opposite side do not have spot size conversion horizontally, and the dimensions of the waveguides are then 3 µm × 3 µm

on the facets as well. Only the side with 11 µm × 3 µm dimensions on the waveguides is used in this work. The layout of the test PIC can be seen in Figure 10 and the side that is used is on the left.

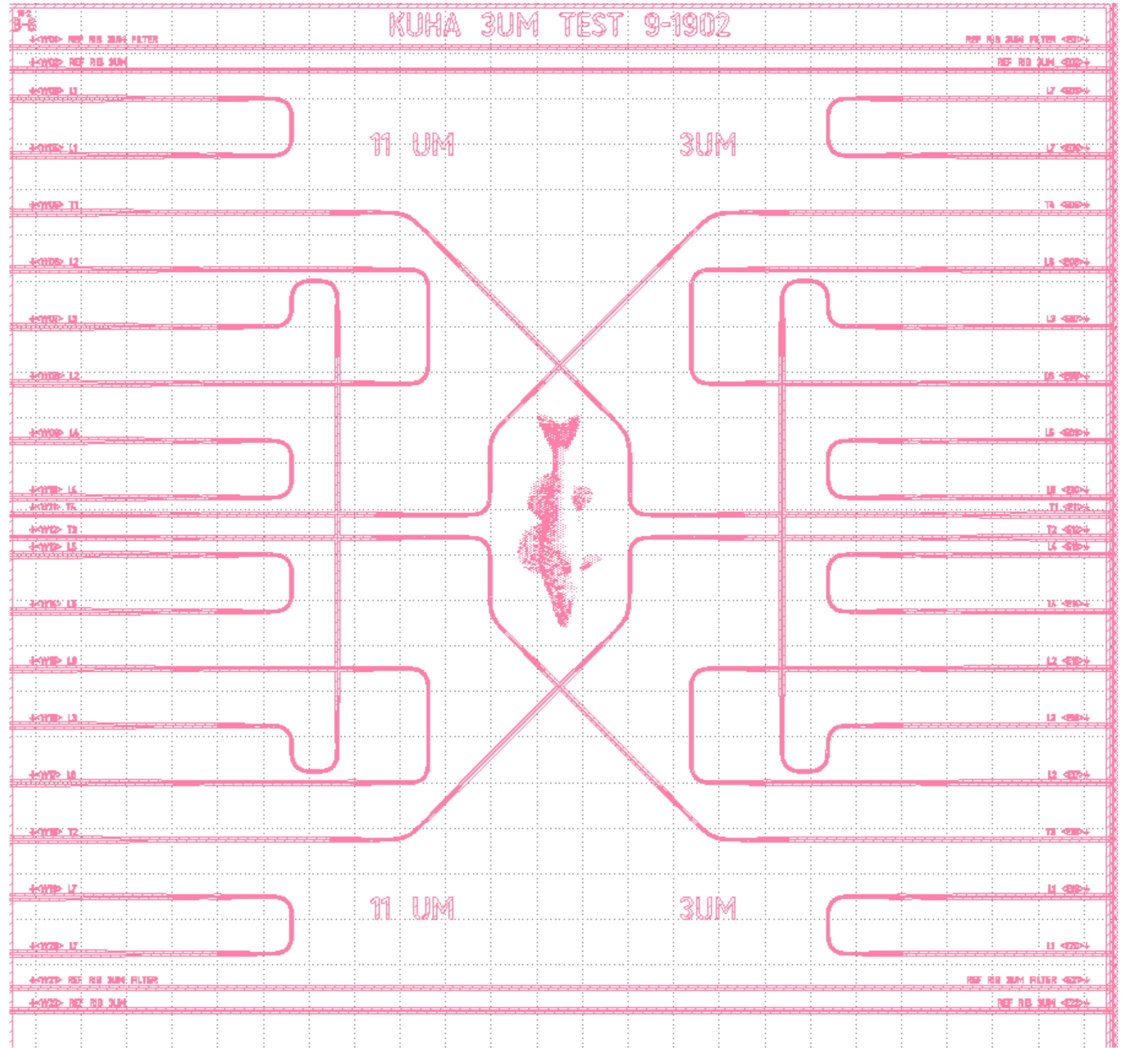

Figure 10. Layout of the test SOI PIC with multiple alignment loops.

The test PIC is glued with silicon rising pads to a copper plate, and a printed circuit board (PCB) is surrounding all its sides except one where the pigtailing is done. There is also an aluminium piece where the strain relief is glued. Figure 11 shows all the parts glued together except the FA and SSC chip. If this test PIC would be one with electrically controlled functions, its electrical wire bonds would go from pads on the chip to the pads on the PCB. Testing of the pigtailing could be done by just gluing the chips straight to the FA, but then there would not be factors affecting the stability of the module like the thermal expansion of all the materials and movements on the fibers.

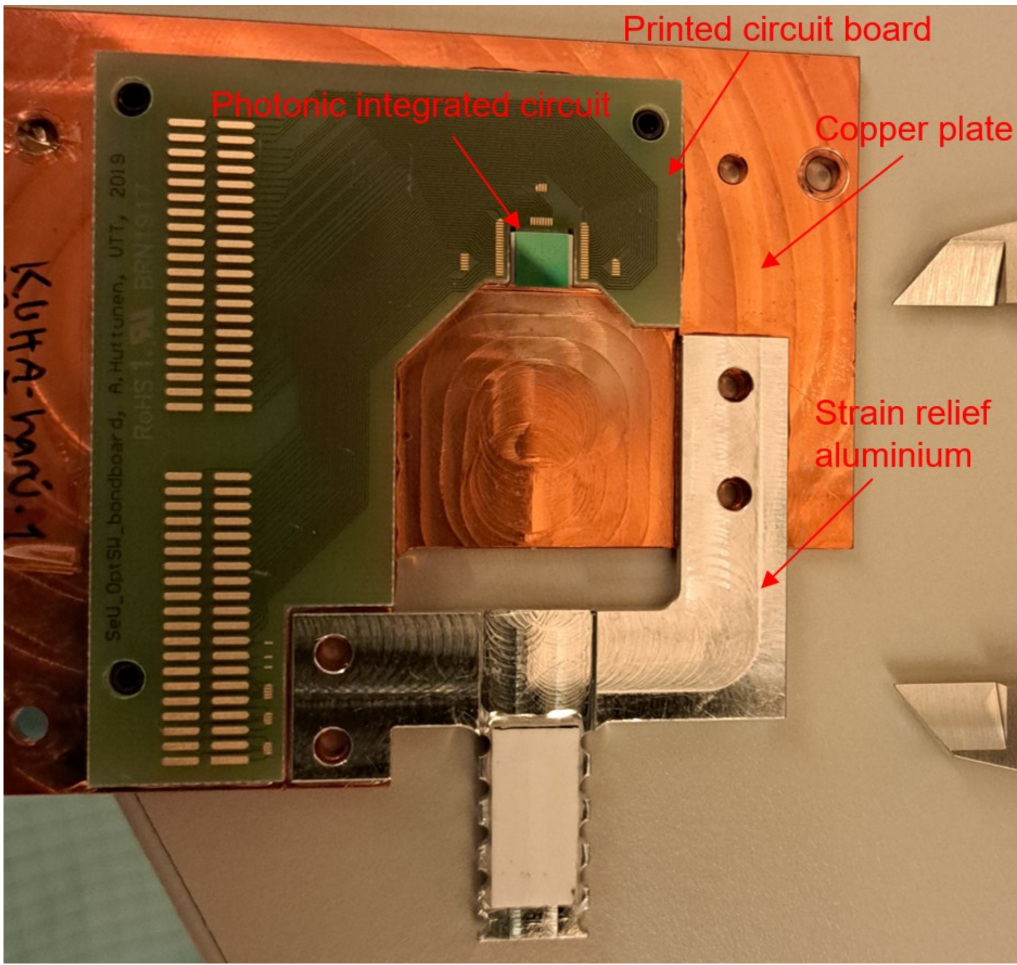

Figure 11. Test PIC on a copper plate.

3 COUPLING PROCESS

Important things while working on this process were to recognize what are all the possible variables that may influence measurement results, coupling losses and long-term stability and reliability of the module. Because the process is slow at this stage, testing out how these variables influence is really time and resource consuming. It is worth it because once the variables and effects are known, the process has fewer steps, or at least they arrive at the result faster and there are fewer mistakes. The whole process could be even automatized or semi-automatized in the future.

3.1 Tools

The most important tool for achieving good results is the computer controlled high precision alignment and assembly station. The assembly station can be seen from Figure 12. With the assembly station and software, it is possible to do the required optical active alignment with numerous scanning algorithms and automations for different parts of the process.

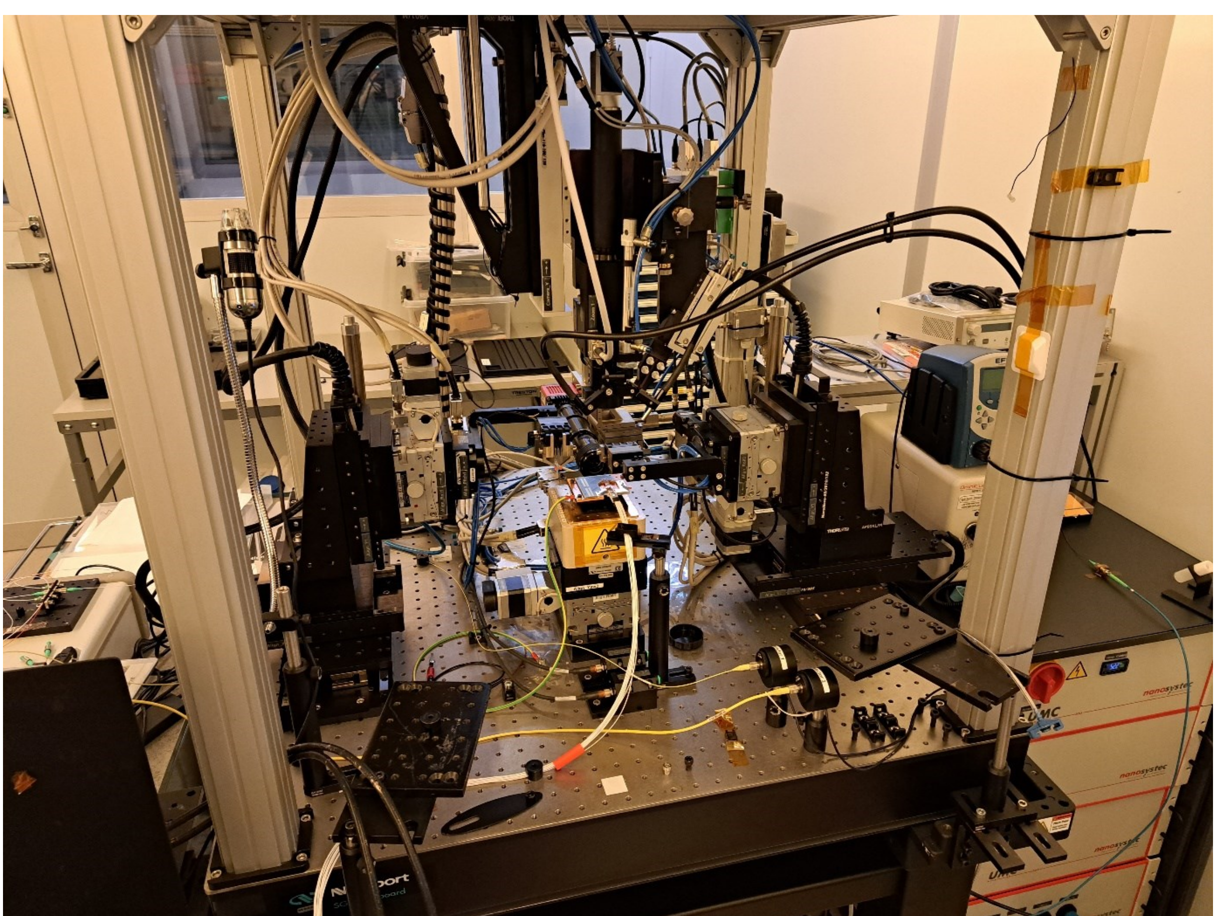

Figure 12. High precision alignment and assembly station.

The assembly station has two aligners which can grip on to fibers / fiber arrays. Both aligners have a force sensor in the gripper that gives relative value for forces in up and down directions.

Between the aligners, there is a tray for the assembly which the fiber array is to be attached. The tray also has a warming element which can warm the surface of the tray up to 100 °C. Figure 13 presents the grippers of the aligners, rehearsal assembly on the tray, and the objective of the infrared camera.

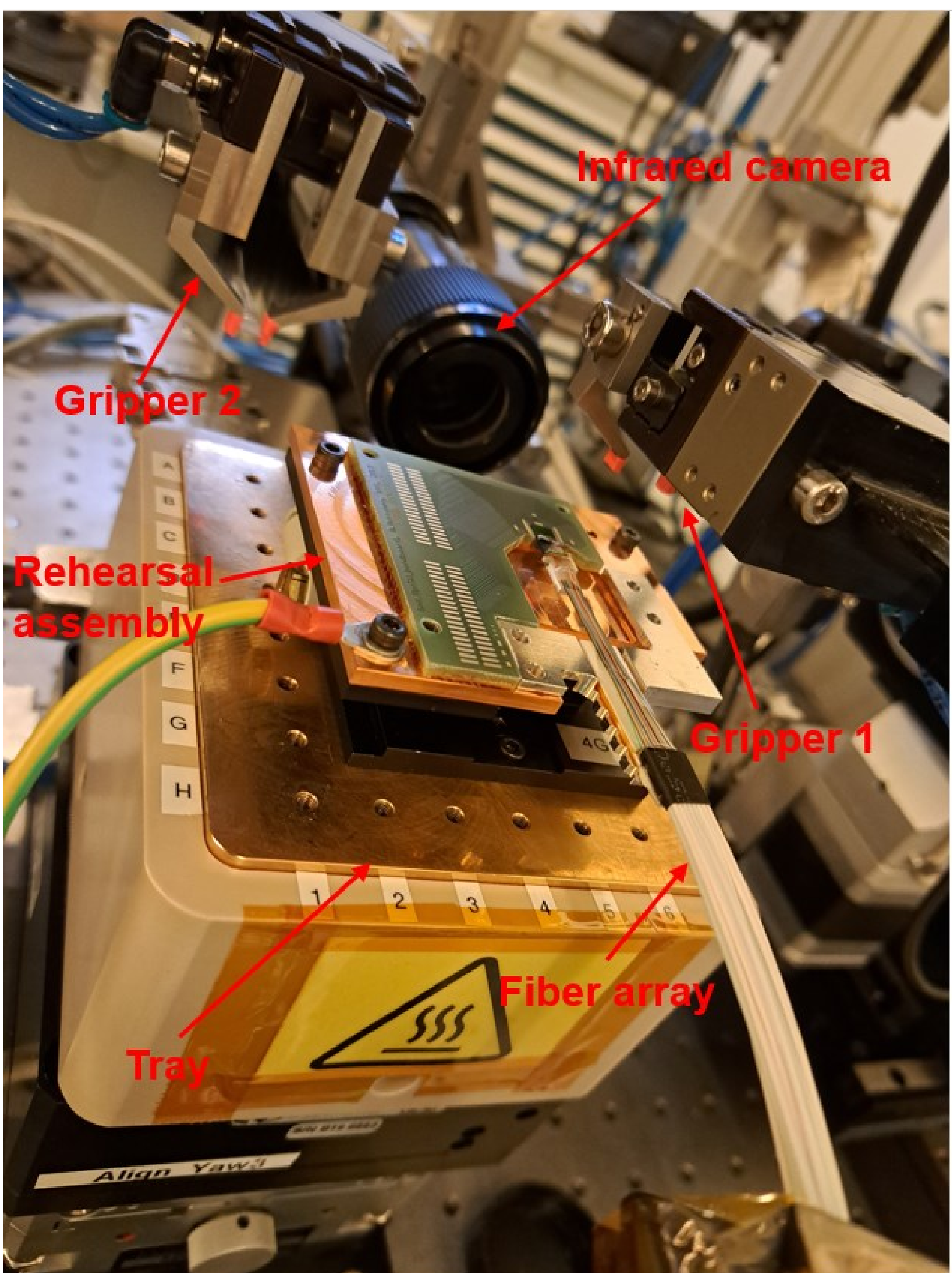

Figure 13. Rehearsal assembly on the tray, two grippers and infrared camera can be seen.

Above the tray, there is a camera which can zoom up to microscopic scales. Camera also has an aligner and it can be moved in x, y, and z directions with good accuracy. Adhesive dispensing syringe and curing light guides can be attached to the same aligner with the camera for accurate dispensing and curing of the adhesives. All the aligners, table and the camera are on a floating optical table for filtering vibrations and movements. Also, the whole assembly station is on four legs that are laying on pillars which are on the concrete base of the building. This minimizes interference from any vibrations coupled from the floor when there are for example people walking close to the machine.

For measuring the optical power and spectrum during the process, two detectors and an optical spectrum analyser are used. The detectors use integrating spheres and Indium Gallium Arsenide (InGaAs) detectors for measuring optical power on a wide spectrum. The measurable power range of the detector is from 1 microwatt (µW) to 1 watt (W) of optical power with 1 nanowatt (nW) resolution. Transimpedance amplifier (TIA) is used to amplifying and converting the output current from the detector into voltage. TIAs are connected with the software of the assembly station for being used as signals for alignment scanning algorithms and converting voltage to optical power to be displayed in charts. Also, an optical spectrum analyser (OSA) is used for measuring. The OSA can measure wavelengths from 600 nm to 1700 nm with the maximum optical power of 10 milliwatt (mW) with ±1 dB power level accuracy. The OSA is not connected to the software of the assembly station.

For making the attachments between fiber arrays and PICs, optical adhesive is used. Properties of the adhesive are very important. Firstly, the light penetrates the adhesive layer between the PIC and fiber array, so the adhesive should have low attenuation and appropriate refractive index for the desired wavelength. Secondly, the adhesive should have low shrinkage because of the required high accuracy alignment, which must stay as close as possible to the point where the maximum optical power is achieved also after the curing of the adhesive. Lastly it should be ultraviolet (UV) light curable for fast curing, and the adhesion on silicon and glass should be good. All these properties should hold for the temperature range that the assembly is to be exposed. Adhesive is cured with UV light source which light guides are attached to the camera aligner of the assembly station for accurate curing.

Super luminescent light emitting diode (SLED) is used as a light source for polarized infrared light to be coupled to the PIC. The SLED is temperature and current controlled. SLED is preferred because of its wide spectrum. The coupling is optimized for the specific spectrum that the used light source provides and using a wide spectrum light source makes a coupling that has good efficiency with different wavelengths.

Other things that are needed in the process are: another light source for UV light that is used for curing the adhesive in the strain relief, IR camera for helping with the first rough alignment, optical isolator for filtering out back reflections towards the SLED, optical splitters for dividing light, microscope, and all the optical fibers that connect fiber arrays to detectors or light source. Optical fibers have the typical insertion loss of 0.3 dB and maximum insertion loss of 0.5 dB.

3.2 Alignment process

The alignment process has many steps, and it would be useful to automate some of them. However, the whole process cannot be fully automated with the equipment in use. Figure 14 shows all the rotations and axial movements that can be done with the assembly station. For achieving low loss coupling three rotations: yaw, pitch, roll, and three axes: y, x, z, should be

in position resulting in the lowest coupling loss for both loops on the left and right sides of the PIC. Aligning a fiber array to a spot size converter has extra steps compared with aligning a fiber array (with SSC attached to it) to a SOI PIC.

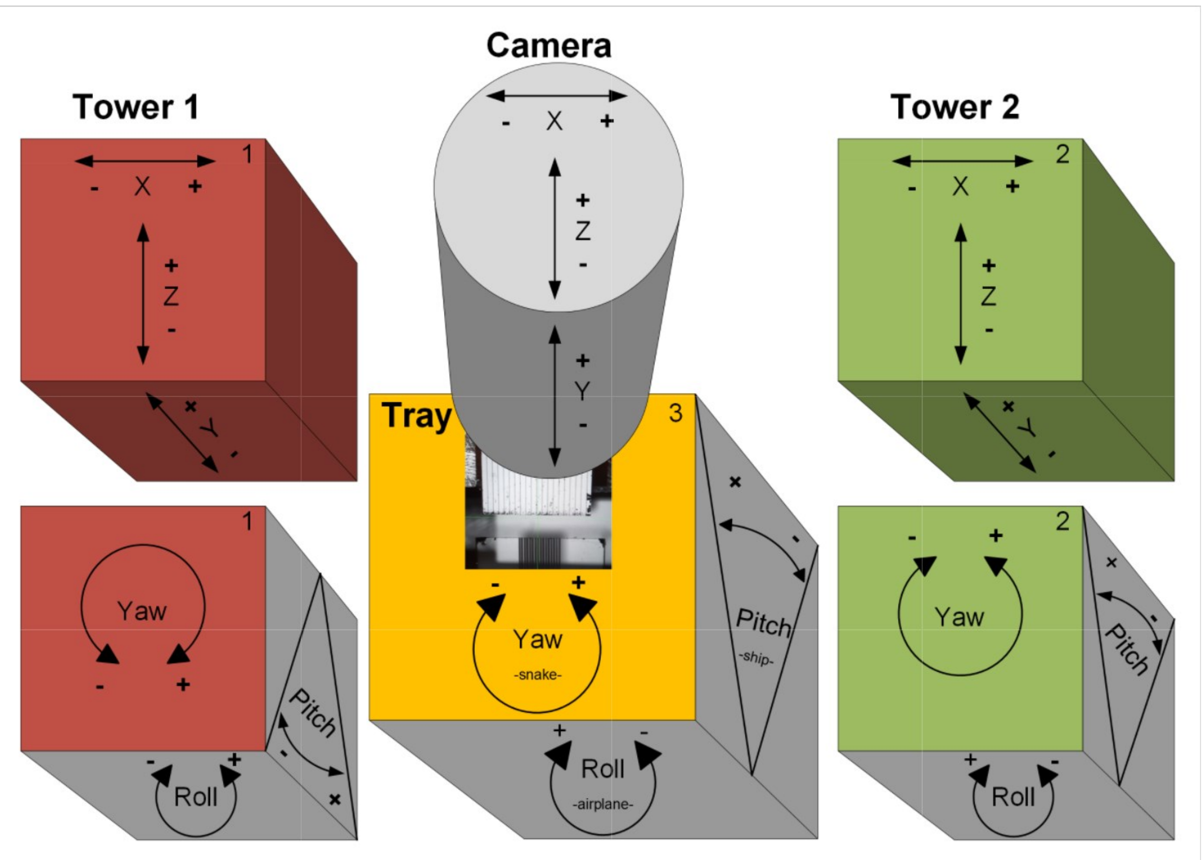

Figure 14. Assembly station which has two aligners, camera, and a tray. Figure made by Brigitte Lanz.

3.2.1 Aligning fiber array to spot size converter

Alignment process of FA to SSC is somewhat more complicated than the second coupling to a functional PIC. This is because SSC has just straight channels and no loops for active alignment, so alignment needs to be made to both sides of the chip, input and output. The SSC chip is also hand polished and there are deviations from intended 90° angles of the waveguide facets. SSC can also support higher order modes. Because of this optimum pitch angle (which results in low coupling to higher order modes) need to be searched between the FA and SSC. This optimum pitch angle has shown to be different when light is coupled to different channels of the SSC, and the biggest difference seems to be with the first channel and the last channel (leftmost channel and rightmost channel).

The process of attaching the FA to the SSC starts with inspecting the fiber array. First the FA is inspected optically with a microscope for particles. If particles are seen, isopropanol alcohol (IPA) and deionized (DI) water are used for cleaning. Drying is done by blowing with nitrogen, so the particles fly away with the liquid. Then the channels of the FA are measured by coupling to another fiber. This way coupling loss differences between channels can be

measured. However, the FA used in this work was already measured by the manufacturer and the differences in the insertion losses could be seen from the test reports. The test reports also include data from all the angles of the v-groove glass corners after polishing which is important information even though usually the tolerances for the angle errors are ± 0.5° from the 90° angles. The real angle from the test report could be included in the calculations with Snell's law for the optimum pitch angle with adhesive. After measuring the optimum pitch angle with an air gap between the FA and the spot size converter the calculation is done. If a FA has a 90.5° angle in the fiber ends, and it is not included in the calculation, the pitch angle would have a difference of ~280 millidegrees (m°) from the optimum angle after the adhesive is applied in the air gap.

After the FA is inspected, the spot size converter chip can be checked similarly with a microscope and be attached to a mounting jig. Once the chip is in place, it could be cleaned with the same methods as the FA.

Cleaned spot size converter chip on a mounting jig is mounted on the tray of the assembly station with a screw. This is when the first, rough alignment process starts. With the top camera view of the assembly station, yaw angle of the tray is adjusted straight relative to the crosshair of the camera view. This can be done visually by looking at the crosshair of the camera view and adjusting the angle so that the horizontal part of the crosshair lines with the chips end. Then the FA can be grabbed with the gripper of the other aligner and moved close to the spot size converter chip. The air gap between the FA and SSC is kept around 50 µm to 100 µm at this point depending on how far from parallel the end of the FA and end of the SSC chip are. Now the yaw angle of the FA can be rotated, at first so that the end of the FA is close to parallel with the crosshair of the camera view. Then final adjustment is done by measuring the air gap distances on the left and right side and using the difference between those lengths to calculate the needed adjustment in degrees. The measuring of the distances is done with the coordinates reported by the aligner of the top camera. The yaw adjustment is illustrated in Figure 15.

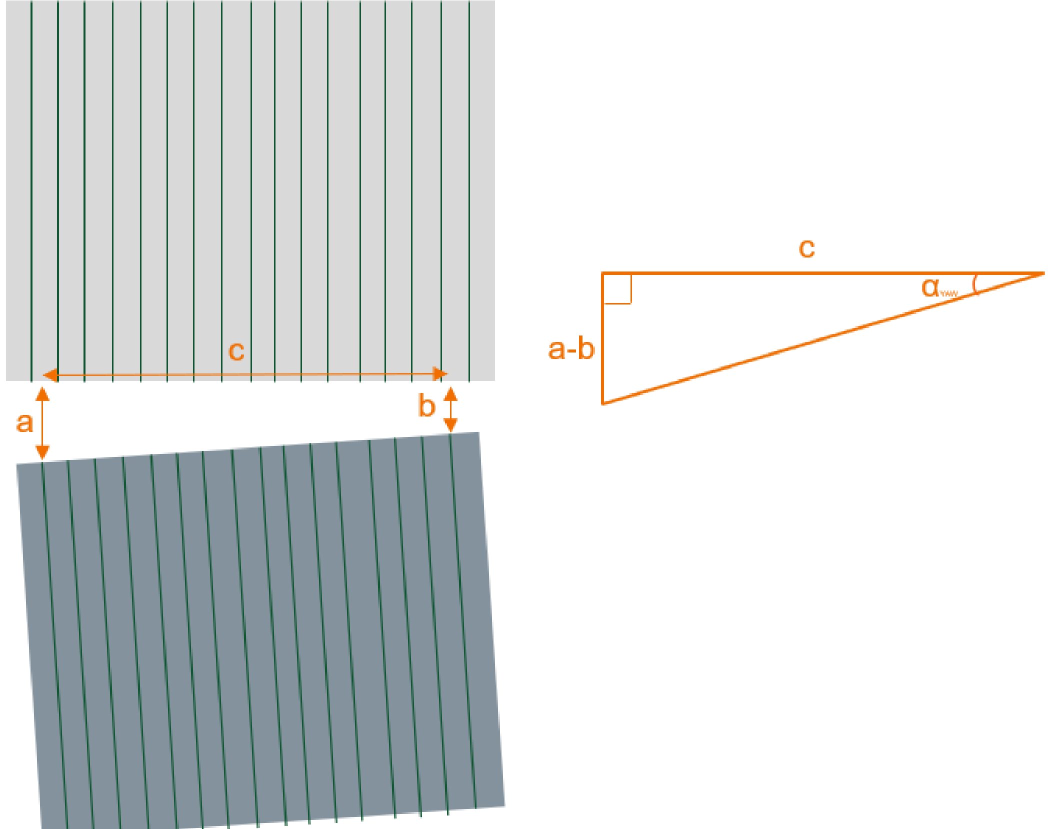

Figure 15. In the figure it is illustrated where *a* and *b* are measured. The length between those measurement points is *c*, and it is known if the measurements are made at the center of a channel. *C* is then pitch multiplied by number of channel spacings between the measurement points. The needed adjustment α_{Yaw} can be calculated using trigonometry.

Equation for the adjustment needed for yaw in degrees is

$$\alpha_{Yaw} = tan^{-1}\left(\frac{a-b}{c}\right), \tag{4}$$

where *a* and *b* are the measured air gap distances in left and right sides of the chip (on channels 1 and 16), *c* is the distance between channels 1 and 16, and α_{Yaw} is the needed adjustment in yaw in degrees. With this method it is possible to make the ends parallel with accuracy of ~50 m°. Even though this is just the first rough alignment process, practice has shown that no adjustments are needed to the yaw angle after this. Because the yaw angle is not adjusted any more, the x direction of the FA is aligned with the channels of the spot size converter using the top camera.

For performing the next steps, a 45° prism mirror is used to get a side view with the top camera. The mirror is carefully rotated so that the crosshair of the top camera aligns with the end of the spot size converter. Then the pitch angle of the FA is adjusted so that it also aligns with the crosshair, and finally the y direction is aligned approximately. The result after this looks like shown in Figure 16. This is named as pitch 0 position. Up to this point alignment has been done without coupling any light to fibers.

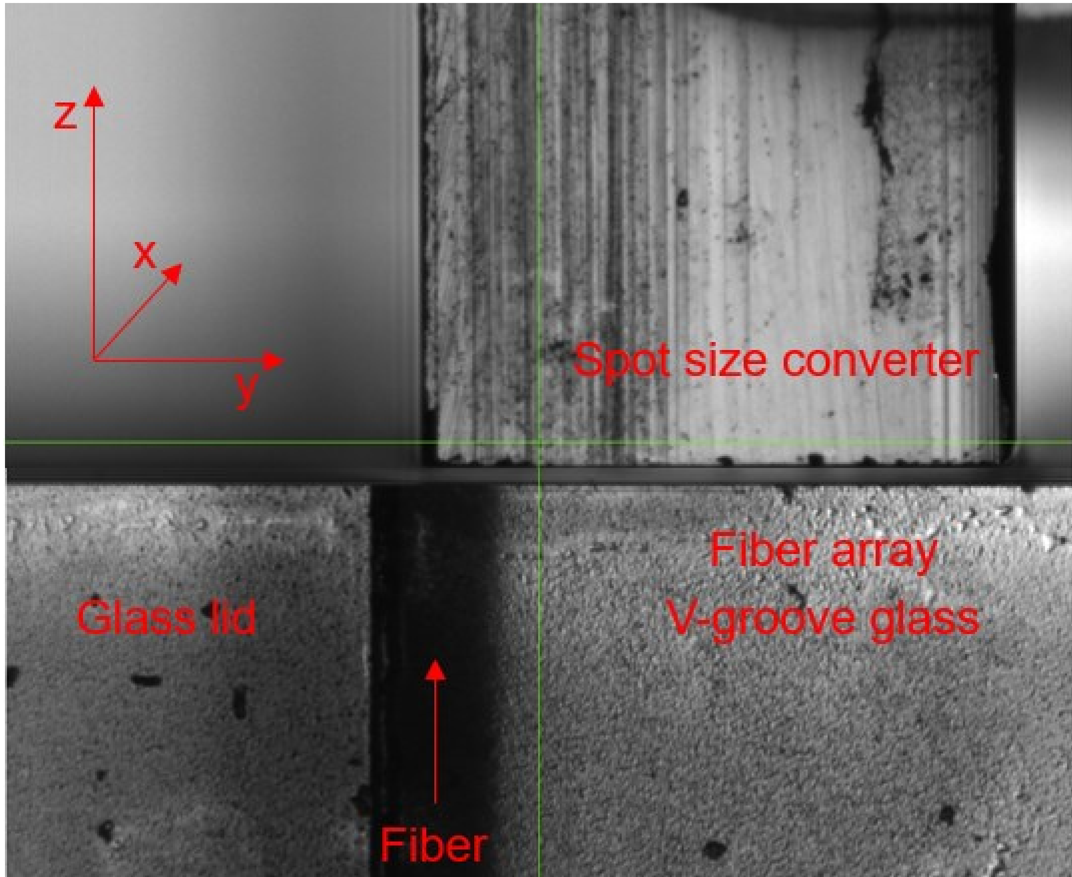

Figure 16. Top camera view of the assembly station through 45° prism mirror, resulting in a side view of the input fiber array and the spot size converter. The ends of the fiber array and spot size converter align with the crosshair of the camera view, resulting in an even air gap between the parts.

Then light from the SLED is split in two with 50:50 splitter and connected to channels 1 and 16 on the FA. Infrared camera is pointed towards the output end of the spot size converter. At this point, every angle except roll is already precisely aligned. From other directions x is roughly in place, y is still to be aligned with the IR camera, and z is minimized lastly which determines the air gap distance. By looking at the IR camera view and moving the y direction of the FA up and down light spots from channels 1 and 16 should be seen where the light comes out from the waveguides of the spot size converter. By looking at the spots at the IR camera view and simultaneously moving the FA up and down, the spots appear brighter and dimmer. Roll is then adjusted so that the spots dim simultaneously at both ends of the spot size converter while moving the FA up and down. Then the roll is roughly aligned, and x and y can be positioned so that the light spots are at their brightest on the IR camera view.

Now that the input side of the spot size converter is aligned roughly, and light is going through the waveguides of the spot size converter and detected by the IR camera in the output, IR camera can be moved away, and a second FA is brought to the output side. The steps for aligning the FA in the output are the same as in input, except that channels 1 and 16 are connected to detectors instead of to the SLED. Then the SLED is switched on and the active alignment starts. By scanning y and x in the output, the signal maximums are searched for both detectors. Roll movement for the output is calculated using the difference between y-coordinates at the maximums for both channels

$$\alpha_{Roll} = tan^{-1}\left(\frac{\Delta Y}{c}\right), \tag{5}$$

where ΔY is the difference between y-coordinates at the maximum output and α_{Roll} is the needed adjustment for the roll in degrees and c is the distance between channels 1 and 16 of the spot size converter. It has turned out to be beneficial to do this at least twice, at first with longer air gap and then almost at contact. Then α_{Roll} can be calculated and adjusted to the input side similarly.

Now the alignment process has been done and the channels of the spot size converter can be measured with the OSA. In the measurement only one channel is used in the output side FA and the channel is always moved to the next channel on the spot size converter. In the input side FA stays in place and channels where the light goes is switched. Output FA channel is connected to a 50:50 splitter and one half goes to a detector and the other half to OSA. Input side is connected straight to the SLED (only the isolator in between). Moving to the next channel on the SSC happens by switching the next connector in the input FA to the light source. Then at the output, FA is moved in x direction by the length of pitch and scanned for the maximum optical power. Figure 17 shows how everything is connected in the measuring setup, a direction of polarization on the input side, and the type of connectors used.

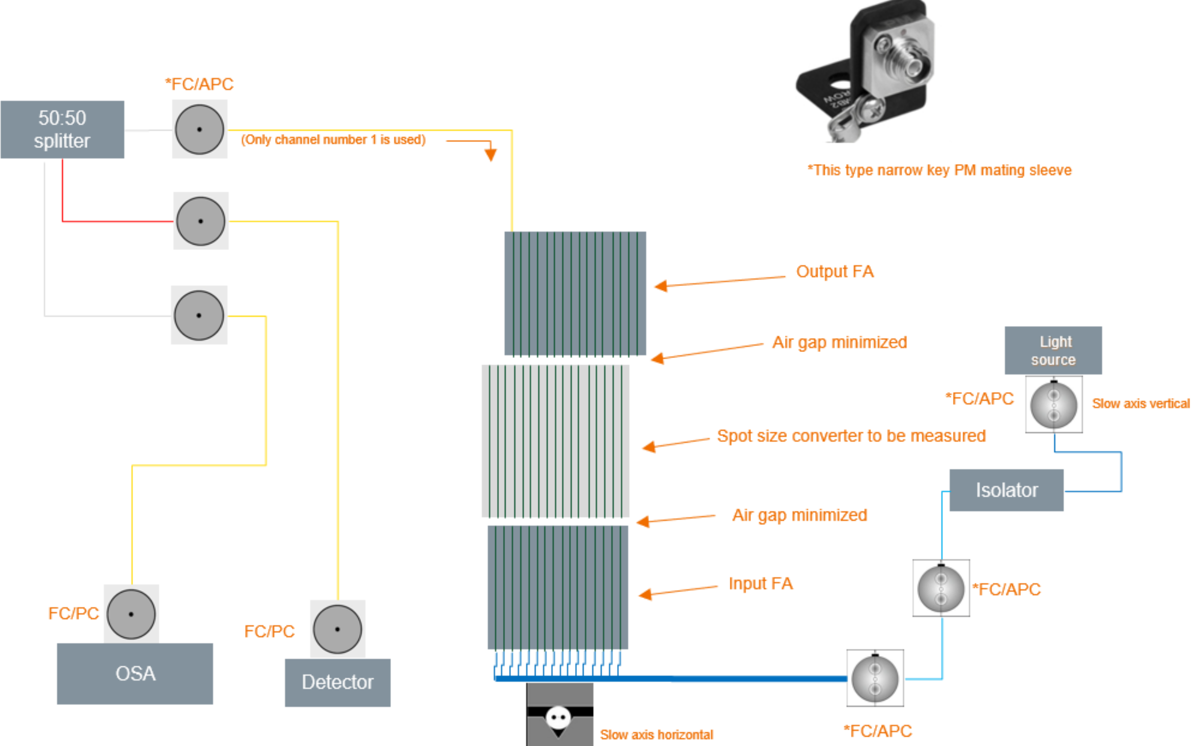

Figure 17. Measuring setup for the spot size converter. Light is coupled from the light source by switching to channels 1-16 of the input fiber array. The one channel on the output fiber array that is in use, is moved to the position where the switched channel of the input fiber array is. The channel of the output fiber array is connected to the optical spectrum analyser and detector of the assembly station using 50:50 splitter.

The following charts show the results of the measurements with different pitch angles for 16 channels in the middle of the spot size converter. The spot size converter has 20 channels but only numbers 3-18 are used. Coupling loss in decibels (dB) is

$$coupling\ loss = -10 \cdot log_{10}\left(\frac{P_m}{P_{ref}}\right), \qquad (6)$$

where P_m is the measured optical power in watts through the device under test and P_{ref} is the measured optical power in watts from the reference. Reference is measured by detaching the connector of channel 1 of the output FA from the splitter input and connecting the fiber from the isolator straight to the splitter instead of input FA.

The first chart (Figure 18) shows the coupling loss as a function of wavelength for channel 3 of the spot size converter with different pitch angles. The goal is to have even and low coupling loss across the bandwidth. According to the chart, the best results are achieved with pitch angle 1000 m° or 1500 m°.

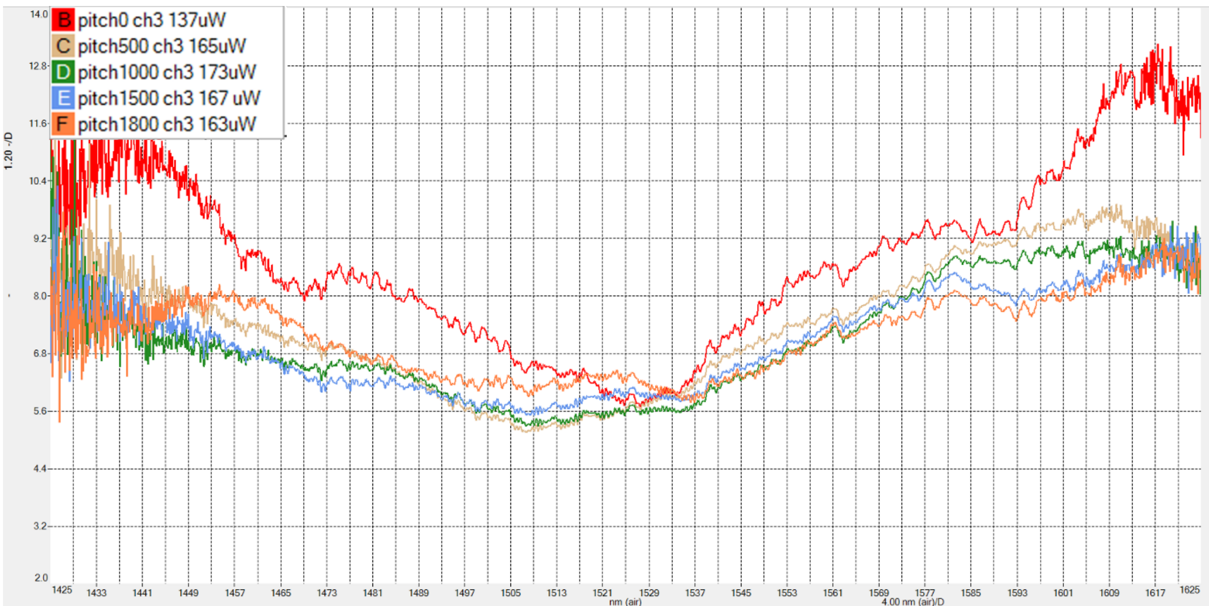

Figure 18. Measurements through channel 3 of the spot size converter with different pitch angles. Y-axis is coupling loss in decibels and x-axis is wavelength in nanometers.

The next chart (Figure 19) shows similarly coupling losses for different pitch angles for the channel 18. From the chart and overall coupling loss it can be seen that the best angle is somewhere between 1500 m° and 2500 m°.

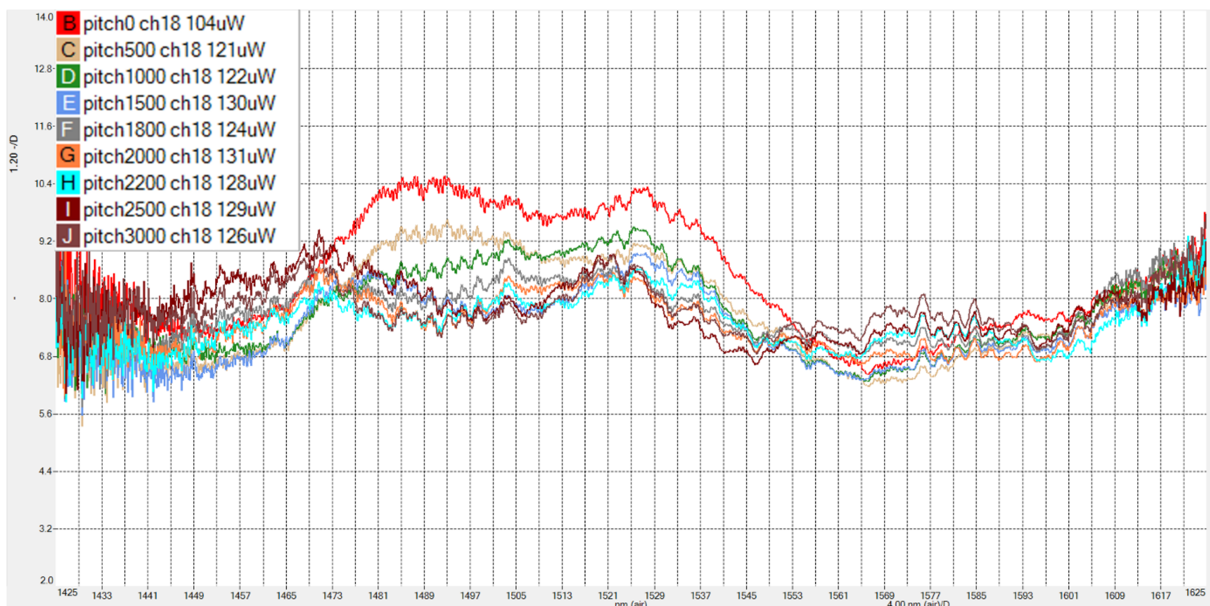

Figure 19. Measurements through channel 18 of the spot size converter with different pitch angles. Y-axis is coupling loss in decibels and x-axis is wavelength in nanometers.

Channels 18 and 3 are on the opposite sides of the chip, and the assumption is that the biggest difference in optimum pitch angle is seen between first and last channel of the spot size converter chip. So, by looking for the optimum pitch angle for the channels at the edges, all the channels between them should also be good with the same angles. Based on the measurements for the edge channels, an angle of 1800 m° is chosen for pitch for all the channels. The next charts (Figure 20 and 21) show coupling losses for 0° and 1800 m° pitch angle for channels 3-18.

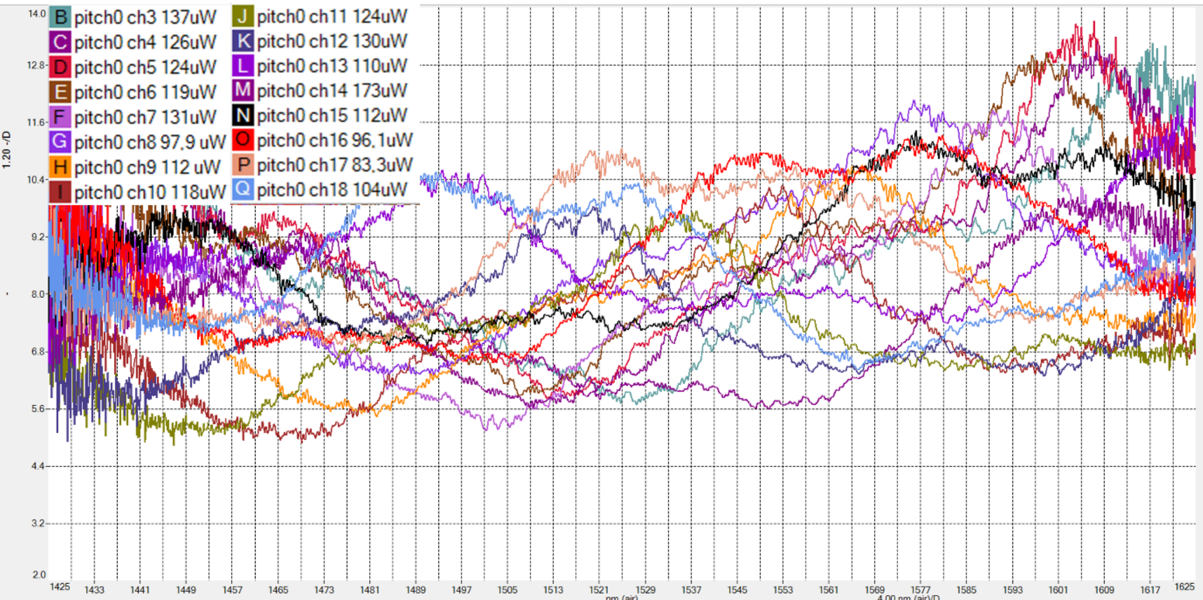

Figure 20. Measurements through channels 3-18 of the spot size converter with pitch 0. Y-axis is coupling loss in decibels and x-axis is wavelength in nanometers.

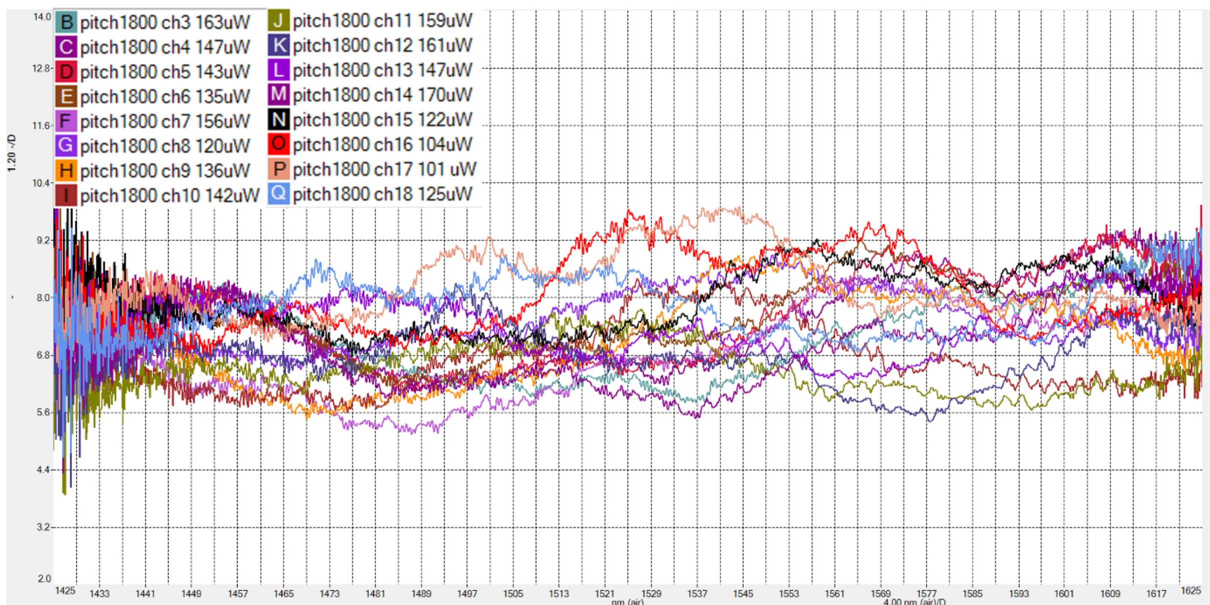

Figure 21. Measurements through channels 3-18 of the spot size converter with pitch 1800 m°. Y-axis is coupling loss in decibels and x-axis is wavelength in nanometers.

The standard deviation of the coupling losses decreased when a 1800 m° pitch angle was used instead of 0°, but the coupling losses are not still even across the bandwidth. Also, when comparing results between channels, differences decreased when 1800 m° was used. There is no other way to improve the coupling losses any more. Next the pitch angle with adhesive is calculated. For this, equation is formed from Snell's law

$$\alpha_{Glue} = sin^{-1}\left(\frac{sin(\alpha_{Air})}{1{,}55}\right) + \left(sin^{-1}\left(\frac{sin(\alpha_{Error})}{1{,}55}\right) - \alpha_{Error}\right), \tag{7}$$

where α_{Glue} is the pitch angle to be used with adhesive, α_{Air} is the optimal pitch angle with air gap that was found in the measurements, and 1.55 is the refractive index of the adhesive and FA in use, α_{Error} is the polish angle reported by the manufacturer of the FA subtracted by 90°. With α_{Air} = 1800 m° and α_{Error} = 30 m°, the result is ~1150 m° with adhesive.

The gluing process is done by switching the output FA to a test SOI PIC, which has loops in the edges. The test chip is glued to an extension arm, which makes more room for the adhesive syringe, because the gripper is not so close to the spot size converter then. A 1150 m° pitch angle is set to the input FA and optical power is measured what is coming back from the loops on both sides of the test chip. Adhesive is applied to the air gap between the FA and spot size converter, and input FA is realigned by scanning x and y to maximum optical power. Then the adhesive is cured with UV light, and once it is cured, the spot size converter is loosened from its mounting jig and moved away with the FA. The following chart (Figure 22) shows the coupling losses of channels 3-18 after the adhesive is cured and the spot size converter is detached from its mounting jig. The output FA is the same SM FA that has been used in all the measurements so far in the output. The same channel 1 of the output fiber array is used for measuring again.

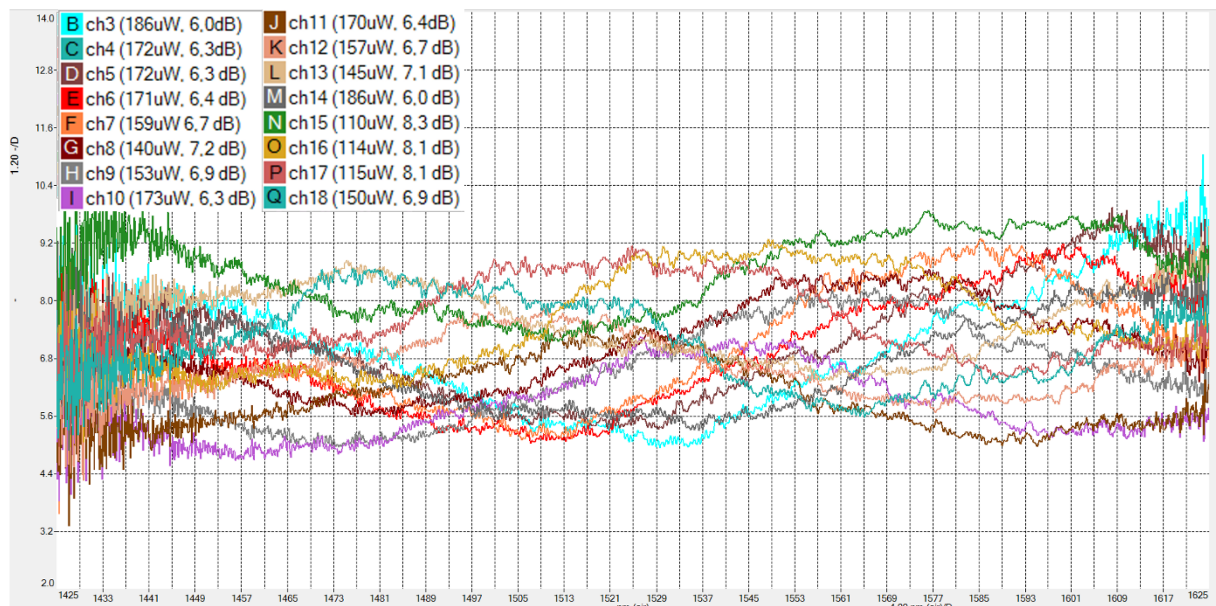

Figure 22. Measurements through channels 3-18 of the spot size converter after curing of the adhesive. Y-axis is coupling loss in decibels and x-axis is wavelength in nanometers.

According to Figure 22 overall coupling losses decreased after curing of the adhesive on almost all channels compared with the measurements with an air gap, but the standard deviations increased from the measurement with an air gap. The decrease in losses could be explained by the decreasing of reflections on the interfaces, because the differences between refraction indices get smaller with the adhesive on the light path. The increase in standard deviations could be explained by a small misalignment that happens during the curing of the adhesive caused by shrinking of the adhesive. Unfortunately, there are no measurement results, where the adhesive would be applied but uncured, and the alignment would be perfect.

3.2.2 Aligning spot size converter to photonic integrated circuit

At this point, the first pigtailing has been done between FA and spot size converter and there is one more to do to the test SOI PIC. The PIC has been attached to a copper plate and it is ready for pigtailing. This part of the process is very similar to the first pigtailing, but there is no need for OSA in this aligning and attaching part. This is because this photonic integrated circuit is not supposed to support higher order modes and the pitch angle can be aligned without active alignment. Nevertheless, when the assembly is ready, OSA is used to make the final measurements.

The first step is to make sure that the chip is clean. If the chip needs cleaning, IPA and DI water are used again with a nitrogen blow dry. Then the PIC which is on the copper plate is attached to the tray of the assembly station and tray yaw is aligned with the crosshair of the top camera. Then with a gripper, FA with the attached SSC is grabbed at the v-groove glass part. After this, the rough alignment process is done just like with the first pigtailing, except IR camera is not used. Instead, light is divided in two from the SLED with a 50:50 splitter and coupled to channels 3 and 18 of the spot size converter. Those channels go to loops 1 and 7 at edges of the test chip (Figure 23).

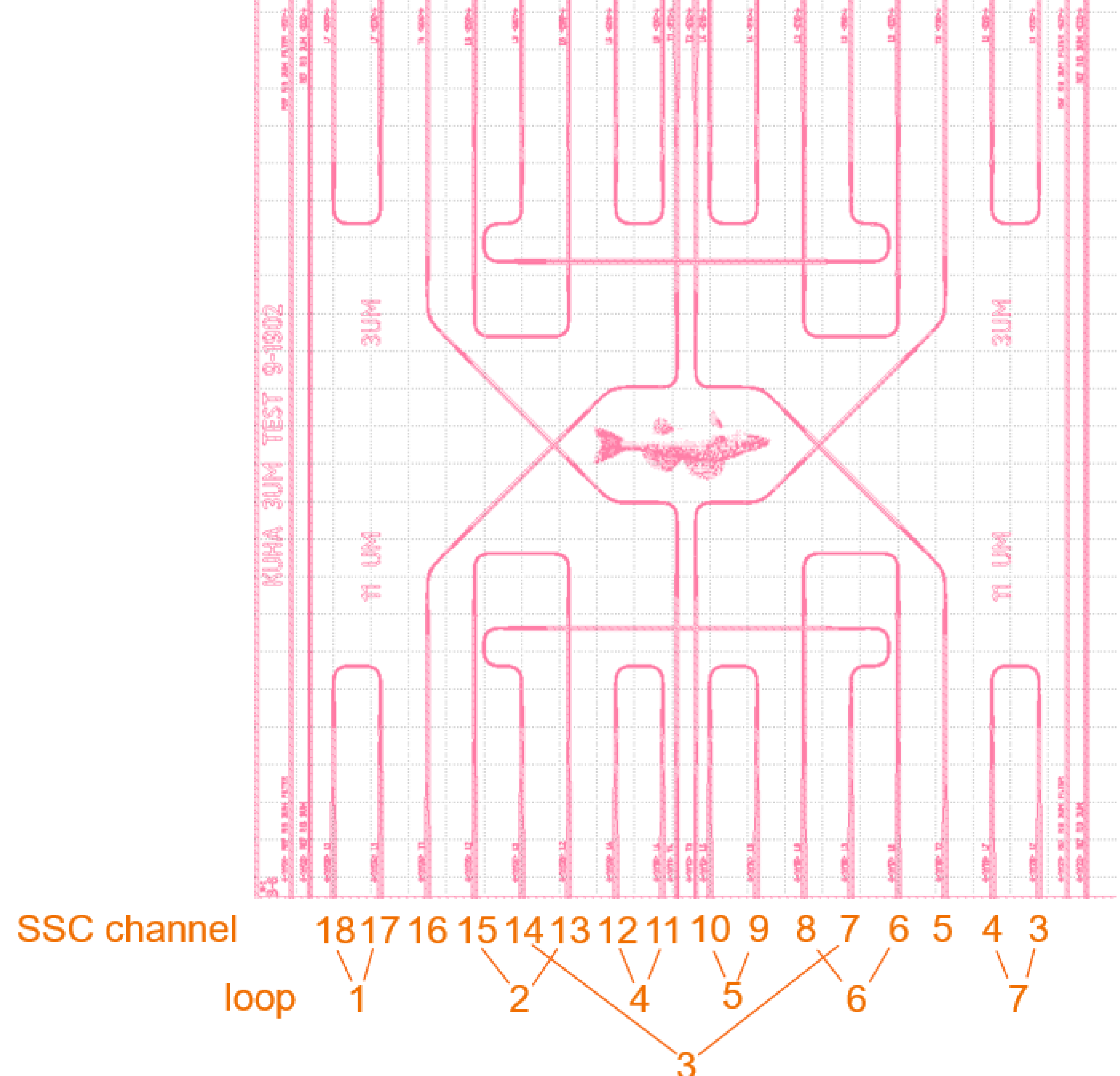

Figure 23. Loops of the test chip are numbered from one to seven. All input and output waveguides of the loops are aligned to different channels of the spot size converter. For example, channel number 15 of the spot size converter is aligned to input of the loop number 2 of the test chip and channel number 13 is aligned to the output of the loop number 2 of the test chip.

Channels 4 and 17 of the spot size converter go to the detectors. Then optical power is maximized to both detectors by adjusting roll with Equation 5. Also, a scanning of x and y must be done to get the optical power maximized along with minimizing the air gap with z. To get the air gap minimized, pitch angle had to be changed from 0° on this chip. The pitch was changed to minus 1800 m° to get the air gap minimized between the SSC and SOI PIC waveguides. Once the alignment is at optimum, the adhesive can be dispensed, and the alignment is done for the last time in x and y direction. Then the adhesive is cured with the UV light.

3.3 Final assembly and measurements

The last step in the process is the finishing of the module so that it is not too fragile. Then the final measurements can be done. Measurements are done last in case of change in optical losses due to releasement of tensions in the adhesive or just defects in the finishing process.

To finish the module, strain relief is glued and the module is protected by a lid or a case. Without strain relief, the coupling would not last the handling of the fibers and connectors during use. Strain relief is glued by attaching the fibers to the aluminium part of the module which was seen in Figure 10. Then a shrink tube is added around the strain relief, and a lid is placed on rising pads and screwed on place so that it hovers over the chips and FA (Figure 24).

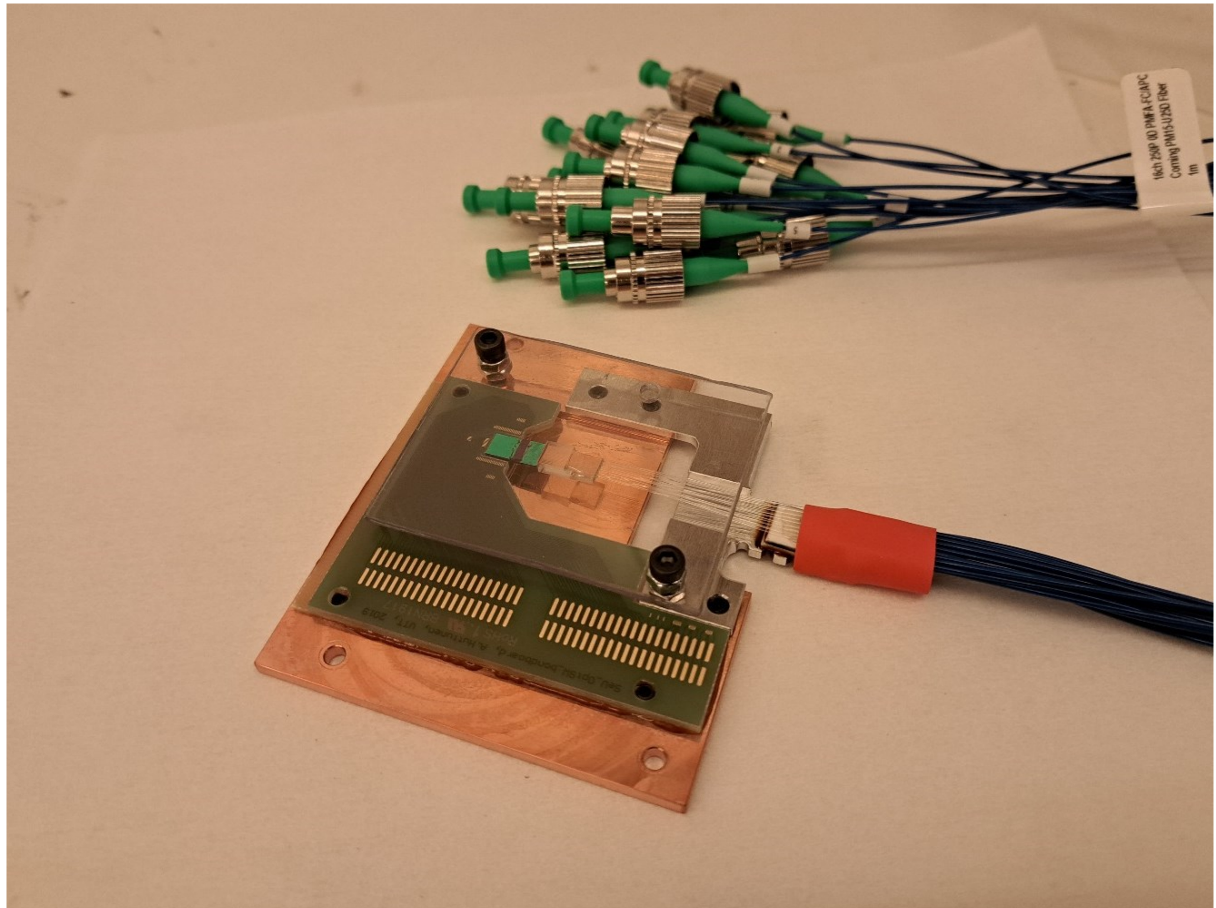

Figure 24. Finished module.

Final measurements can be made without using any splitters. Light from the SLED is connected to any loop and the other end is coupled straight to OSA. Reference is measured straight from the source (isolator in between). Figure 25 shows the coupling losses as a function of wavelength for loops 1-7 on the test chip. Overall coupling losses for the loops are also calculated and can be seen in the legend names.

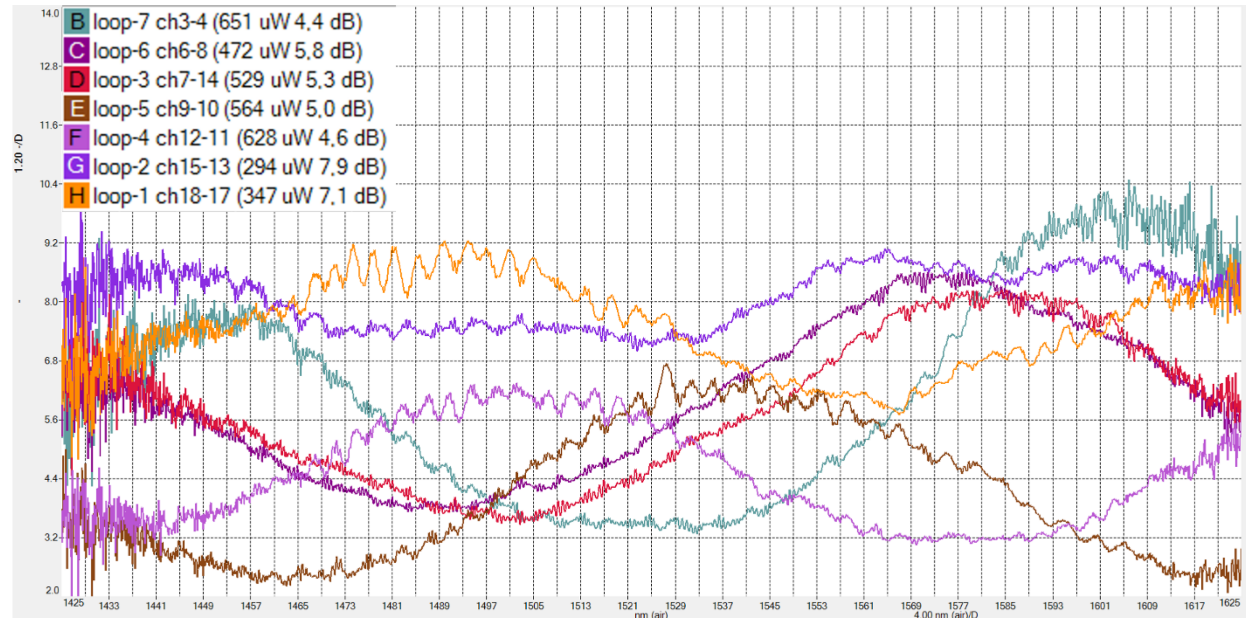

Figure 25. Final measurements from the loops of the test chip after finishing the module. Y-axis is coupling loss in decibels and x-axis is wavelength in nanometers.

According to Figure 25, the differences in coupling losses between loops are remarkably high. Also, the coupling losses of the loops are wavelength dependent and there are not much consistencies between the loops. Overall coupling losses were 4.4 dB for the best loop which was number 7 and 7.9 dB for the worst loop which was number 2.

After the final measurements, the assembly has been baked in 60 °C for 12 hours and in 80 °C for 12 hours and no changes have been observed in the results. Also, by moving the fibers or tapping the v-groove glass with tweezers have no influence in coupling losses.

4 DISCUSSION

Mechanical stability of this kind of assembly seems acceptable, but further testing should be done. Coupling losses are not affected by moving the module or the fibers. Tapping the v-groove glass with tweezers do not make a difference. Also, after 12 hours of baking in 80 °C the results stay the same. The coupling loss results are not good enough for low loss coupling to all channels. There might be multiple reasons for this, and several possible reasons are discussed after the problem is properly introduced with the charts.

To simplify the reviewing, the results are limited to loops 1 and 7 on the test SOI PIC and their channels on the spot size converter. The chart in Figure 26 (and chart seen in Figure 21 for all channels) indicates that the coupling is not the only factor causing differences between channels on the finished module. The differences were already seen from the measurements at start when the coupling was optimal. Defects in the spot size converter, in the input FA, or in the connectors could be the explanations for the differences between these curves (Figure 26).

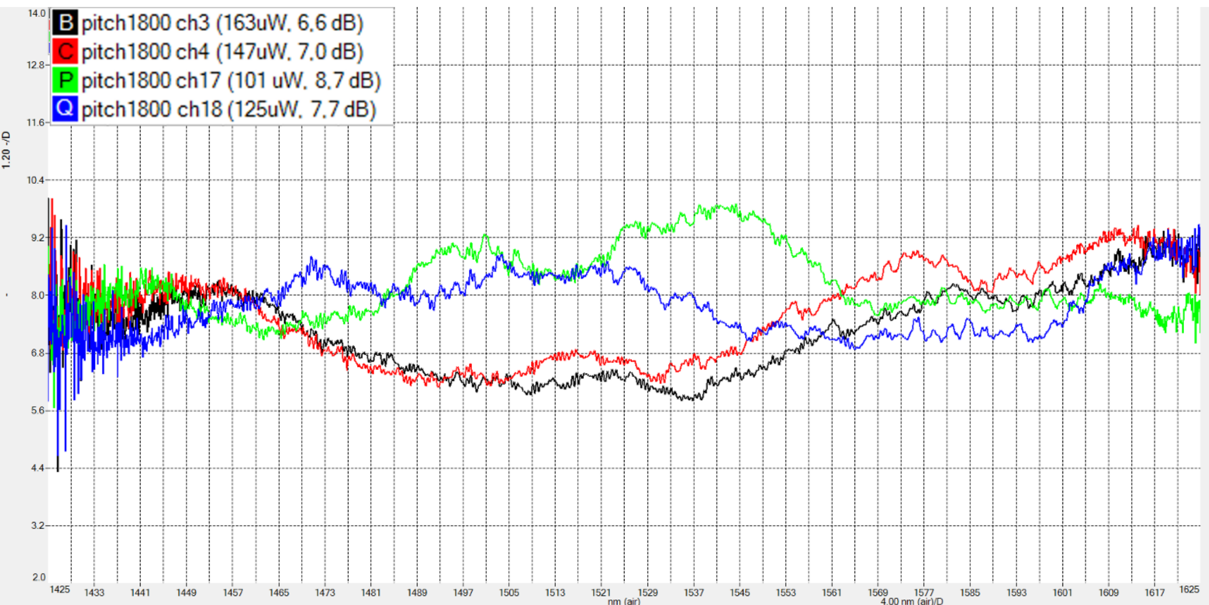

Figure 26. Coupling losses as a function of wavelength for channels going to loops 1 and 7 on the test SOI PIC. Measurement was done without adhesive and with the best possible pitch angle for both channels 3 and 18. Y-axis is coupling loss in decibels and x-axis is wavelength in nanometers.

The best-case scenario would be that the coupling loss would be the same across the bandwidth. The angle on the 11 µm waveguide facets of the spot size converter and the difference in this angle between channels could be the cause of the wavelength dependency. This is because with a fiber array only one pitch angle can be chosen, and it cannot be the best possible pitch angle for all the channels. Also, it could be that the waveguide facet is not on the same angle across the whole of its height as illustrated in Figure 27.

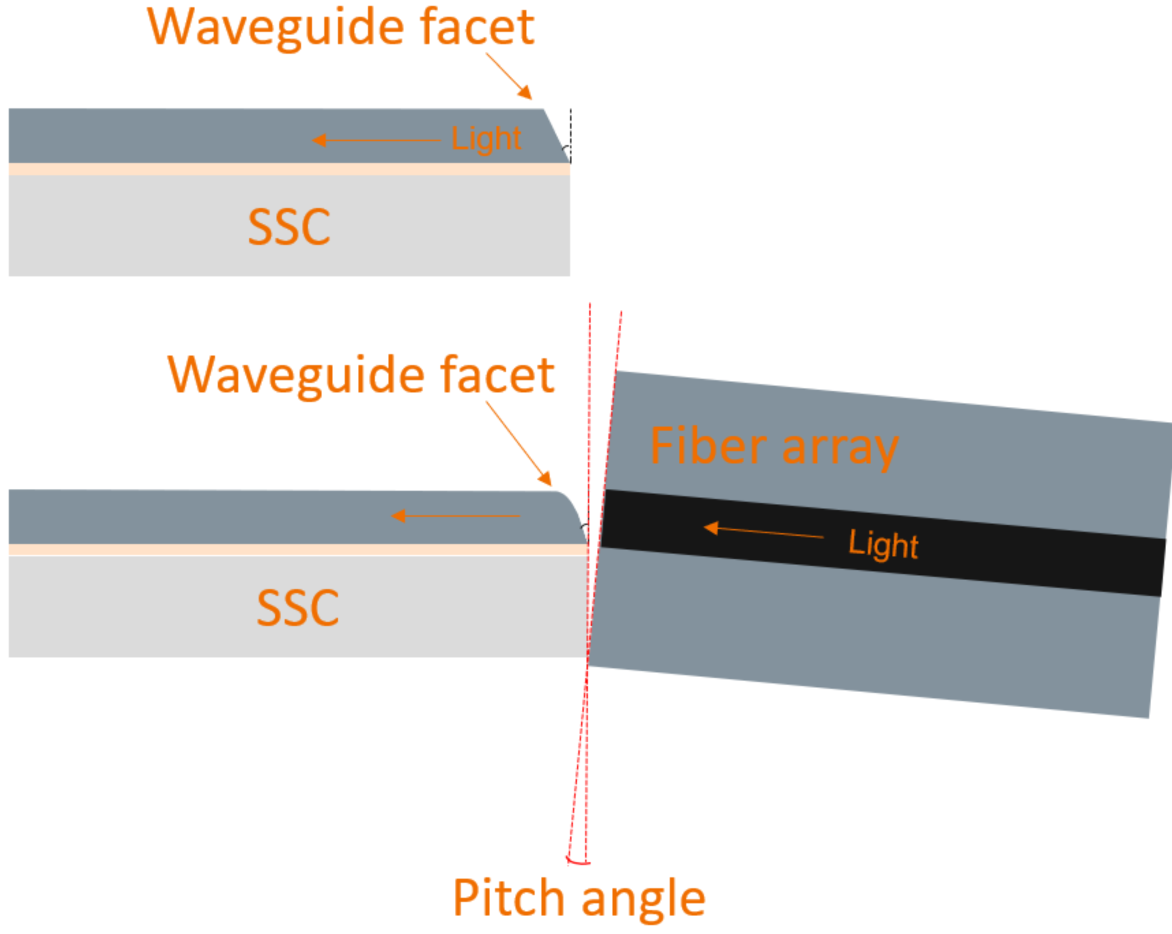

Figure 27. Top: Spot size converter waveguide with an angle on its facet. Bottom: Spot size converter waveguide with an angle and rounded corner on its facet. (Not in scale and angles are exaggerated.)

The angle on the waveguide facets of the spot size converter was also observed differently than measuring. It was impossible to close the air gap between the spot size converter and the test SOI PIC with pitch angle 0°. This is because the test SOI PIC facets are similarly polished as in the SSC and most probably have the same kind of angle on waveguide facets. That is why the pitch angle needed to be set at least to minus 1800 m° to close the air gap.

From the results, the coupling losses are not the same with channels 3 and 18 on the spot size converter even if their own optimum pitch angles are used. The reason for this could be the difference in a numerical aperture on the channel that has more angle and rounding on the facet. Addition to this because the fiber array touches the bottom edge of the SSC chip, the air gap is then longer with a larger pitch angle. Also, the more the facet is rounded the larger part of the optical power might couple to higher order modes even if the optimum pitch angle is used.

Another challenge is potential misalignment during the curing. As mentioned earlier, this is only assumed based on optical power values during the curing, no spectra are available from the stage where the adhesive is applied but uncured. Therefore, hardly any conclusions can be made from measurement results if the misalignment during curing only rises overall coupling losses or also changes the shape of the spectra. Figure 28 shows the charts for channels 3-4 and 17-18 of the SSC after the adhesive is cured.

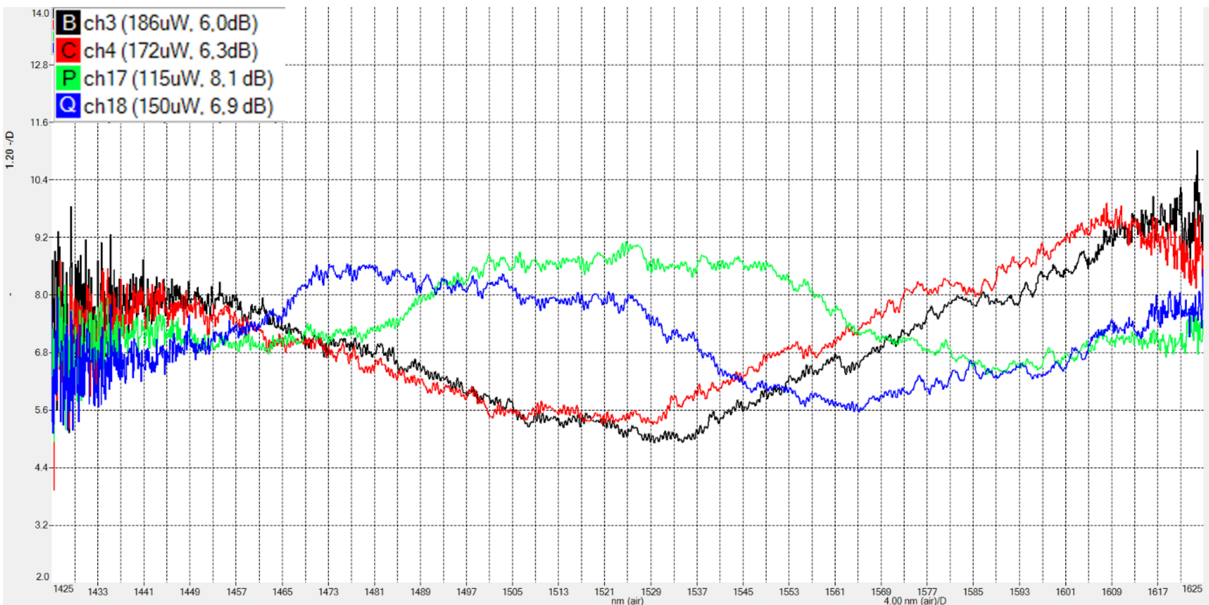

Figure 28. Coupling losses as a function of wavelength after adhesive curing for channels on the spot size converter going to loops 1 and 7 on the test SOI PIC. Y-axis is coupling loss in decibels and x-axis is wavelength in nanometers.

The overall coupling losses dropped from the measurements with an air gap to measurements with cured adhesive. In the fiber array to the spot size converter, the drop was 0.6 dB on channel 3, 0.7 dB on channel 4, 0.6 dB on channel 17, 0.8 dB on channel 18. If all channels (3-18) are reviewed, the value of improvement in overall coupling losses caused by the gluing of FA to SSC is 0.45 dB on average. The best case was channel 6 with 1.0 dB improvement and the worst was channel 15 with 0.4 dB worsening. If there would not be any misalignment caused by the curing of the adhesive, the coupling losses should improve more than 0.45 dB on average. This is because the reflections decrease on the interfaces, and pitch angle is smaller than what was with the air gap. Interesting is why a 0.4 dB increase in losses was measured in channel 15 when there are 0.4 dB decreases on its neighbour channels. The misalignment should increase coupling losses quite equally especially on channels next to each other so it cannot be explained with that. A possible explanation could be a particle on optical path or a loose connector. Also, there is a reason to suspect that the optical fiber which is used to connect the light to different channels on the FA is worn out and it has maximum insertion loss greater than 0.5 dB causing differences in measurement results every time it is reconnected.

Figure 29 shows the charts for loops 1 and 7 after the assembly is ready. When comparing charts from Figure 28 and Figure 29 must be remembered that in Figure 28 light travels through an air gap from SSC to the output FA, and in Figure 29 there is no air gap but the light travels through a loop and comes back on some other channel on the SSC and input FA. Also, in Figure 29 the gluing to SOI PIC has already been made and the misalignment has happened.

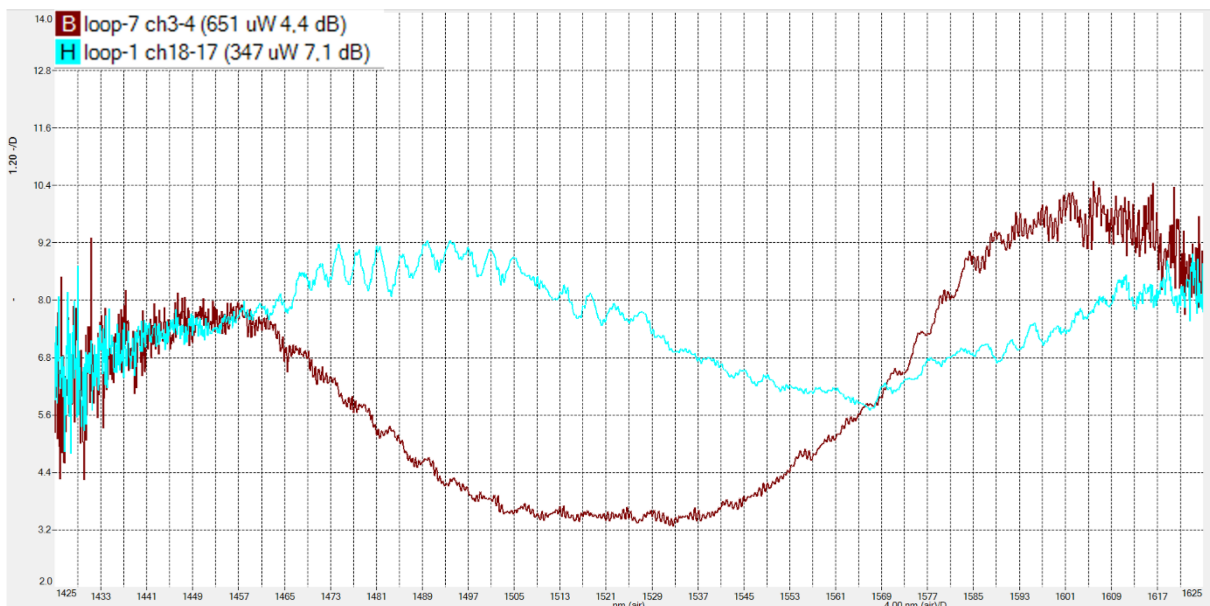

Figure 29. Coupling losses as a function of wavelength after the assembly is ready for loops 1 and 7 on the test SOI PIC. Y-axis is coupling loss in decibels and x-axis is wavelength in nanometers.

Even though the two measurements are made with a different setup, it is interesting to compare the results. There is some information that could be gathered about differences between channels. Also, the difference with measurement results with the air gap and the measurement results with cured adhesive. If it is assumed that coupling losses are the same for both directions on the light path, the coupling losses on Figure 28 could be added together to get the coupling loss for the whole path that light takes going through the loop. With the SOI PIC in the output of the SSC, smaller coupling losses are achieved because the mode field diameters match better than with the SM FA. However, it could be calculated that SSC channels going to loop 1 had the overall coupling loss of 8.1 dB + 6.9 dB = 15 dB and channels going to loop 7 had 6.0 dB + 6.3 dB = 12.3 dB before the pigtailing to the SOI PIC. After the pigtailing losses were 7.1 dB for channels going to loop 1 and 4.4 dB for channels going to loop 7. So, then both loops 1 and 7 had 7.9 dB improvement. By making the same calculation to all loops the best improvement was in loop 4 with 8.5 dB improvement, and loop 3 had the least improvement with 7.4 dB. The reviewing of overall coupling losses calculated like this can be seen from Table 1 where the starting point with a trade off pitch angle is also included by summing up two channels on the SSC that go to a loop together.

Table 1. Overall coupling losses compared through the process

loop	**before first pigtailing**	**after first pigtailing (FA to SSC)**	**difference made with first pigtailing**	**after second pigtailing (SSC to SOI PIC)**	**difference made with second pigtailing**
1 (ch18-17)	16.4 dB	15.0 dB	-1.4 dB	7.1 dB	-7.9 dB
2 (ch15-13)	14.9 dB	15.4 dB	+0.5 dB	7.9 dB	-7.5 dB
3 (ch7-14)	13.2 dB	12.7 dB	-0.5 dB	5.3 dB	-7.4 dB
4 (ch12-11)	13.3 dB	13.1 dB	-0.2 dB	4.6 dB	-8.5 dB
5 (ch9-10)	14.6 dB	13.2 dB	-1.4 dB	5.0 dB	-8.2 dB
6 (ch6-8)	15.3 dB	13.6 dB	-1.7 dB	5.8 dB	-7.8 dB
7 (ch3-4)	13.6 dB	12.3 dB	-1.3 dB	4.4 dB	-7.9 dB

5 SUMMARY

This work studied a coupling method and resulting coupling losses of a photonics module composed of a silicon-on-insulator (SOI) photonic integrated circuit, a 16-channel single mode fiber array and a spot size converter chip. The converter chip was used to optimize the coupling efficiency between the fiber array and the SOI circuit by matching the mode field diameter of the fiber array to that of the SOI circuit. The SOI circuit had multiple 180° loop waveguides to facilitate active alignment by optical loss measurements during assembly. An active alignment method was used for the input and output couplings of the converter chip using, a 1536 nm super luminescent light emitting diode (SLED) as a light source, an ultraviolet light curable adhesive and a computer controlled high precision alignment and assembly station. As a result, light travels through the fiber array and the spot size converter to the 180° optical loops on the SOI circuit and after that back to the fiber array through the spot size converter.

The goal of this thesis was to achieve reliable, low loss coupling within the bandwidth of a 1536 nm SLED. The underlying theory was reviewed and a measurement setup was implemented. The high precision assembly station was the single most important tool. Further development was made to the existing alignment process to obtain an optimal result.

The best result for coupling loss through a 180° loop on the SOI PIC was 4.4 dB and the worst was 7.9 dB on the final assembly. The stability of the coupling was found acceptable, but further testing should be done on that. The elementary proof tests such as baking in 80 °C, mechanical tapping, or various ways to move or bend the module and its parts did not affect the coupling losses. Improvements were made in comparison with earlier results achieved with the same components, but the loss results did not meet the goals. The goal was less than 4.5 dB coupling loss measured through a loop.

The multimode behaviour of the spot size converter and the effect of angles in the waveguide facets needed a lot of attention because these effects had not been studied much before. The conclusion was that the facet angle variation on the spot size converter and a worn-out optical fiber were the main factors causing the differences between the channels. Thus, research in all these subjects continues. Other factors such as misalignment during curing of the adhesive might also have some effect on differences in optical losses between channels though it should have had equal effect on all channels. The data gained from this study will be useful for the future improvements of the coupling process and the chip fabrication.

6 REFERENCES

[1] Saleh B.E.A., Teich M. C. (1991) Fundamentals of Photonics, John Wiley & Sons, Inc., 949 p.

[2] Fiber optics for sale, (read 20.3.2023) URL: https://www.fiberoptics4sale.com/blogs/wave-optics/waveguide-modes.

[3] Bogaerts W., Selvaraja S. K. (2011) Compact Single-Mode Silicon Hybrid Rib/Strip Waveguide With Adiabatic Bends. IEEE Photonics Journal, vol. 3, no. 3, pp. 422-432

[4] Johnson S.G., Povinelli M.I., Soljacic M., Karalis A., Jacobs S., Joannopoulos J.D. (2005) Roughness losses and volume-current methods in photonic-crystal waveguides. Appl. Phys. B 81, 283–293

[5] Bogaerts W., Baets R., Dumon P., Wiaux V., Beckx S., Taillaert D., Luyssaert B., Van Campenhout J., Bienstman P., Van Thourhout D. (2005) Nanophotonic waveguides in silicon-on-insulator fabricated with CMOS technology. In Journal of Lightwave Technology, vol. 23, no. 1, pp. 401-412, January.

[6] Bogaerts W., Selvaraja S. K. (2014), Silicon-on-insulator (SOI) technology for photonic integrated circuits (PICs): Silicon-On-Insulator (SOI) Technology Manufacture and Applications, Cambridge, England ; Waltham, Massachusetts: Woodhead Publishing.

[7] Streshinsky M., Ding R., Liu Y., Novack A., Galland C., Lim A. E. -J. Guo-Qiang Lo P., Baehr-Jones T., Hochberg M. (2013) The Road to Affordable, Large-Scale Silicon Photonics.

[8] Carroll L., Lee J. -S., Scarcella C., Gradkowski K., Duperron M., Lu H., Zhao Y., Eason C., Morrissey P., Rensing M., Collins S., Hwang H. Y., O'Brien P. (2016) Photonic Packaging: Transforming Silicon Photonic Integrated Circuits into Photonic Devices.

[9] Marchetti R., Lacava C., Carrol L., Gradkowski K., Minzioni P. (2019) Coupling strategies for silicon photonics integrated chips.

[10] Design Guidelines for Photonic Integrated Circuit Packaging, (read March 2023) URL: www.phix.com.

7 APPENDICES

Appendix 1 Polarization maintaining fiber datasheet (PM 1550)
Appendix 2 Datasheet of the light source

Appendix 1 Polarization maintaining fiber datasheet (PM 1550)

PANDA PM

High Performance Polarization Maintaining Fibers

Specialty Optical Fibers

PANDA PM Specialty Fibers are designed with the best polarization maintaining properties, and are the industry standard in the world today. The fibers offer low attenuation and excellent birefringence for high performance applications. Available in a wide range of standard operating wavelengths up to 1550 nm, and with a variety of coating designs, PANDA PM Specialty Fibers are optimal for high performance polarization retaining fiber applications. This field-proven fiber supports high growth applications, and performs well over a wide temperature range.

Applications

- High performance transmission laser pigtails
- Polarization-based modulators
- High data rate communications systems
- Polarization-sensitive components
- Raman amplifiers
- Fiber optic sensors, gyroscopes and instrumentation

PANDA PM Specialty Optical Fiber design uses two stress applying parts to create an extremely high birefringence, resulting in fiber with excellent polarization maintaining properties. This design was invented and patented by Corning Incorporated. Corning continues to have a manufacturing partnership with Fujikura Ltd.

Key Optical Specifications for All Coatings

	PM 1550	PM14XX	PM 1310	PM 980	PM 850	PM 630	PM 480	PM 400
Operating Wavelength (nm)	1550	1400-1490	1310	980	850	630	480	410
Cutoff Wavelength (nm)	1300-1440	1260-1380	1130-1270	870-950	650-800	520-620	400-470	330-400
Maximum Attenuation (dB/km)	0.5	1.0	1.0	2.5	3.0	12	30	≤ 50
Mode-field Diameter (µm)	10.5 ± 0.5	9.8 ± 0.5	9.0 ± 0.5	6.6 ± 0.5	5.5 ± 0.5	4.5 ± 0.5	4.5 ± 0.5	3.5 ± 0.5
Beat Length Range (mm)	3.0-5.0	2.8-4.7	2.5-4.0	1.5-2.7	1.0-2.0	≤ 2.0	≤ 2.0	≤ 1.7
Maximum Cross Talk @ 100 m (dB)	-30	-30	-30	-30	-30	-30	-30	-30*
Typical Cross Talk @ 4 m (dB)	-40							

*PM 400 Cross Talk is -30dB/100 m at 410 nm and 480 nm measurement wavelengths

M0500017
Issued: January 2019
Supersedes: May 2018

Appendix 2 Datasheet of the light source

THORLABS

Benchtop Superluminescent Light Source

S5FC1550S-A2

Description

The Thorlabs Fiber Coupled SLD Source provides easy coupling and simple control of a Superluminescent Diode (SLD). Each system is equipped with a single FC/APC connector output. The drive electronics feature an independent, high-precision, low-noise, constant-current source and a temperature control unit. An intuitive LCD interface allows the user to view and set current and temperature parameters independently. The S5FC includes a universal power supply allowing operation over 100 to 240 VAC without the need for selecting the line voltage and is supplied with a US line cord as well as a standard European line cord. The fuse access is conveniently located on the rear panel. The SLD offered here is an indium phosphide (InP) device coupled to a SM fiber. For added safety, the system is designed to meet 3B laser class requirements.

SLDs are excellent high power broadband light sources for use as ASE Light Sources and in applications like Optical Coherence Tomography (OCT) Imaging Systems and Fiber Optic Gyroscopes (FOG).

Specifications

General Specification	Value
AC Input	100 - 240 VAC, 50 - 60 Hz
Input Power	20 VA Max
Fuse Ratings	250 mA
Fuse Type	IEC60127-2/III (250 VA, Slow Blow Type 'T')
Fuse Size	5 mm x 20 mm
Dimensions (W x H x D)	5.8" x 11.4" x 2.6" (146 mm x 290 mm x 66 mm)
Weight	5 lbs (9.1 lbs Shipped Weight)
Operating Temperature	15 to 35 °C
Storage Temperature	0 to 50 °C
Connections and Controls	
Interface Control	Optical Encoder with Pushbutton
Enable Select	Keypad Switch with LED Indicator
Power On	Key Switch
Fiber Ports	FC/APC
Display	LCD, 16 x 2
Input Power Connection	IEC Connector
Modulation Input Connector	BNC (Referenced to Chassis)
Interlock	100 mil Header
Communications	
Communications Port	USB 2.0
Com Connection	USB Type B Connector
Required Cable	2 m USB Type A t B Cable (Replacement Item # USB-A-79)

Specifications Subject to Change without Notice

May 9, 2012
22887-S01, Rev C

Specifications Continued

Optical Specifications			
	Min	Typical	Max
Operating Current	-	550 mA	600 mA
Center Wavelength	1520 nm	1550 nm	1580 nm
ASE Power	2 mW	2.5 mW	-
Optical Bandwidth	85 nm	90 nm	-

Performance Specifications	
Current Set Point Resolution	0.1 mA
Temperature Adjust Range	20 to 30 °C
Temp Set Point Resolution	± 0.01 °C
Noise, (Typ Source Dependent)	<0.1%
Rise Time / Fall Time	1.4 µsec / 1.6 µsec
Modulation Input	0-5 V = 0 - Full Power
Modulation Bandwidth	250 KHz Full Depth of Modulation

Drawings